

On Erlang mixture approximations for differential equations with distributed time delays*

Tobias K. S. Ritschel[†]

Abstract. In this paper, we propose a general approach for approximate simulation and analysis of delay differential equations (DDEs) with distributed time delays based on methods for ordinary differential equations (ODEs). The key innovation is that we 1) propose an Erlang mixture approximation of the kernel in the DDEs and 2) use the linear chain trick to transform the resulting approximate DDEs to ODEs. Furthermore, we prove that the approximation converges for continuous and bounded kernels and for specific choices of the coefficients if the number of terms increases sufficiently fast. We show that the approximate ODEs can be used to assess the stability of the steady states of the original DDEs and that the solution to the ODEs converges if the kernel is also exponentially bounded. Additionally, we propose an approach based on bisection and least-squares estimation for determining optimal parameter values in the approximation. Finally, we present numerical examples that demonstrate the accuracy and convergence rate obtained with the optimal parameters and the efficacy of the proposed approach for bifurcation analysis and Monte Carlo simulation. The numerical examples involve a modified logistic equation, chemotherapy-induced myelosuppression, and a point reactor kinetics model of a molten salt nuclear fission reactor.

Key words. Mixture approximations, distributed time delays, delay differential equations, linear chain trick.

MSC codes. 37M05, 39B99, 41A30, 65D15, 65P99, 65Q20

1. Introduction. Many industrial and natural processes exhibit time delays [30], e.g., due to advection (flow in a pipe or river), diffusion (mixing), or feedback mechanisms (natural or man-made), and as time delays can have a significant impact on the dynamics and stability of a process [37], it is important to account for them when developing and analyzing mathematical models. Such models typically involve differential equations, and the time delays can either be absolute (discrete) or distributed (continuous) [50]. In the former case, the right-hand side function depends on the state at specific points in the past, and in the latter, it depends on a weighted integral of all past states, i.e., a convolution. The weight function is called the kernel or memory function. Although discrete time delays are more commonly used, they typically arise from a simplification of the underlying phenomena. For instance, assuming plug-flow in a pipe leads to an absolute time delay whereas a nonuniform flow velocity (e.g., Hagen-Poiseuille flow) leads to a distributed delay [43]. In this work, we focus on the latter.

In recent decades, there has been a significant interest in distributed time delays, and they have been used to model a variety of processes, e.g., in pharmacokinetics and pharmacodynamics (PK/PD) [23], neuroscience [1], side-effects of chemotherapy [33], the Mackey-Glass system [36, 57], which can describe respiratory and hematopoietic diseases, population models in biology [8, 13], and pollution in fisheries [6]. Mechanical [2] and economic [17] processes have also been considered, and we refer to the book by Kolmanovskii and Myshkis [30] for

*Submitted to the editors 03/14-2026.

[†]Department of Applied Mathematics and Computer Science, Technical University of Denmark, DK-2800 Kgs. Lyngby, Denmark (tobk@dtu.dk).

more examples. Furthermore, many theoretical results have been developed specifically for DDEs with distributed time delays. Rahman et al. [42] studied the stability of networked systems with distributed delays, Yuan and Belair [55] present general stability and bifurcation results, Bazighifan et al. [4] analyze oscillations in higher-order DDEs with distributed delays, Cassidy [7] demonstrate the equivalence between cyclic ordinary differential equations (ODEs) and a scalar DDE with a distributed delay, and Aleksandrov et al. [3] study the stability of systems with state-dependent kernels.

Despite the many applications, there exists far less theory and fewer numerical methods and software for DDEs with distributed time delays than for ODEs. Even for DDEs with absolute delays, there exist many numerical methods [5, 39] and significant amounts of off-the-shelf software, e.g., for simulation [49]. However, some modeling software does contain functionality for distributed time delays, e.g., NONMEM [54] and Phoenix [23], and customized numerical methods have also been proposed. Typically, they 1) approximate the integral in the convolution using a quadrature rule, e.g., a trapezoidal [24] or Gaussian [51] rule, and 2) discretize the differential equations using a one-step method, e.g., a Runge-Kutta method [57, 16] or a linear multistep method [52]. Methods based on splines have also been proposed [58]. However, compared to similar methods for ODEs, approximating the convolution is requiring in terms of computations and memory, and it is not straightforward to choose the time step size adaptively.

Consequently, it is desirable to identify approaches that can directly take advantage of existing theory, methods, and software for ODEs, and for a specific class of kernels, it is possible to transform DDEs with distributed delays to ODEs. Specifically, the transformation is called the *linear chain trick* (LCT) [35, 40, 50], and it is applicable when the kernel is given by the probability density function of an Erlang distribution (referred to as an Erlang kernel). See also [12] on sufficient and necessary conditions under which DDEs can be transformed to ODEs. The LCT has been widely used, and Hurtado and Kiro Singh [25] and Hurtado and Richards [26, 27] generalized it to transform a wider range of stochastic mean field models to ODEs. Additionally, both Cassidy et al. [9] and Krzyzanski [32] have proposed to simplify the simulation and analysis of specific DDEs by approximating the involved gamma kernels by a hypoexponential kernel and a truncated binomial series, respectively, and Guglielmi and Hairer [18] consider exponential mixture approximations and demonstrate their approach for DDEs involving both gamma and Pareto kernels. However, to the best of the author's knowledge, Erlang mixture approximations of general continuous and exponentially bounded kernels have not previously been combined with the LCT to approximate DDEs with distributed time delays by ODEs.

Therefore, in this work, we present a general-purpose Erlang mixture approximation for continuous and bounded kernels, which allows us to use the LCT to approximate a large class of DDEs with distributed time delays by ODEs. In recent work, this approximation was used to develop an algorithm for identifying kernels in DDEs based on partial measurements of the state [44]. We prove that 1) the mixture approximation converges, 2) the approximate ODEs can be used to assess the stability of the steady states of the original DDEs, and 3) the solution to the ODEs converges to that of the DDEs. Furthermore, we propose a least-squares approach for determining the Erlang mixture approximation coefficients and rate parameter. We use numerical examples to demonstrate that such an optimal approximation is more accurate

than an approximation which uses theoretical coefficients from the proof, and we compare with the accuracy of one of the exponential mixture approximations described by Guglielmi and Hairer [18] for the model in [32]. Finally, using two numerical examples, we demonstrate that the proposed approach can be used to approximately simulate and analyze the solution of DDEs with distributed time delays.

The remainder of the paper is structured as follows. In Section 2 and 3, we present the notation used and the system considered in this paper, respectively. Next, we present the main theoretical results of the paper in Section 4, and in Section 5, we describe the least-squares approach. In Section 6 and 7, we present numerical examples, and conclusions are presented in Section 8.

2. Preliminaries. The spaces $\mathbb{R}_{\geq 0} = \{x \in \mathbb{R} | x \geq 0\}$ and $\mathbb{N}_{\geq 0} = \{0, 1, \dots\}$ contain the non-negative real numbers and integers, respectively, and $\mathbb{R}_{> 0} = \{x \in \mathbb{R} | x > 0\}$ and $\mathbb{R}_{\leq 0} = \{x \in \mathbb{R} | x \leq 0\}$ are the spaces of positive and non-positive real numbers. We denote by \odot the Hadamard (or elementwise) product (also called the Schur product) [21, 22], i.e., if $c = a \odot b$, then $c_i = a_i b_i$. Furthermore, $\det A$ is the determinant of the matrix argument, A , and $\text{diag } a$ denotes a diagonal matrix whose diagonal elements are the elements of the vector (or set) argument, a , i.e., if $C = \text{diag } a$, then $C_{ii} = a_i$ and $C_{ij} = 0$ for $i \neq j$. We will use the ∞ -norm defined by

$$(2.1) \quad \|a\|_{\infty} = \max \{|a_i|\}_{i=1}^n, \quad \|A\|_{\infty} = \max \left\{ \sum_{j=1}^m |A_{ij}| \right\}_{i=1}^n$$

for a vector $a \in \mathbb{R}^n$ and a matrix $A \in \mathbb{R}^{n \times m}$. If $A = \text{diag } a$ is diagonal, then $\|A\|_{\infty} = \|a\|_{\infty}$. We will make repeated use of the identity

$$(2.2) \quad e^{at} = \sum_{m=0}^{\infty} \frac{(at)^m}{m!}$$

in the proofs in Section 4, and we denote by $[\cdot]^+ = \max\{0, \cdot\}$ the positive part of the argument.

The main theoretical results of the paper are related to convergence [48, Chap. 7]. A function $f_n : \mathbb{R}_{\geq 0} \rightarrow \mathbb{R}$ converges *pointwise* to $f : \mathbb{R}_{\geq 0} \rightarrow \mathbb{R}$ (i.e., $f_n(x) \rightarrow f(x)$) as $n \rightarrow \infty$ if there exists an $N : \mathbb{R}_{\geq 0} \rightarrow \mathbb{N}$ for every $\epsilon \in \mathbb{R}_{> 0}$ and $x \in \mathbb{R}_{\geq 0}$ such that $|f_n(x) - f(x)| < \epsilon$ for all $n > N(x)$. If N can be chosen independently of x , the convergence is *uniform*. We will also show results on *weak* convergence, i.e., that the integral converges: $\int_0^x f_n(y) dy \rightarrow \int_0^x f(y) dy$ as $n \rightarrow \infty$. Finally, we will also show convergence of the absolute difference (convergence in L^1 -norm): $\int_0^{\infty} |f_n(x) - f(x)| dx \rightarrow 0$ as $n \rightarrow \infty$. We will also use the result that if $f_n(x) \rightarrow g_n(x)$ and $g_n(x) \rightarrow f(x)$ as $n \rightarrow \infty$ where $g_n : \mathbb{R}_{\geq 0} \rightarrow \mathbb{R}$, then $f_n(x) \rightarrow f(x)$ as well because the error can be bounded through a triangle inequality: $|f_n(x) - f(x)| = |f_n(x) - g_n(x) + g_n(x) - f(x)| \leq |f_n(x) - g_n(x)| + |g_n(x) - f(x)|$. Both terms can be made arbitrarily small. In particular, we will use this result together with Stirling's approximation [46]: $\ln n! \approx n \ln n - n + \frac{1}{2} \ln 2\pi n$. The error of this approximation decreases with $1/n$, i.e., the approximation converges as $n \rightarrow \infty$. The concepts are similar if n is a real number instead of a natural number and if the domain and range of f_n , g_n , and f are different.

3. System. We consider systems in the form

$$(3.1a) \quad x(t) = x_0(t), \quad t \in (-\infty, t_0],$$

$$(3.1b) \quad \dot{x}(t) = f(x(t), z(t)), \quad t \in [t_0, t_f],$$

where $t \in \mathbb{R}$ is time, $t_0, t_f \in \mathbb{R}$ are the initial and final time, $x : \mathbb{R} \rightarrow \mathbb{R}^{n_x}$ is the state, and $x_0 : \mathbb{R} \rightarrow \mathbb{R}^{n_x}$ is the initial state function. Furthermore, $f : \mathbb{R}^{n_x} \times \mathbb{R}^{n_z} \rightarrow \mathbb{R}^{n_x}$ is the right-hand side function, and the memory state, $z : \mathbb{R} \rightarrow \mathbb{R}^{n_z}$, is given by the convolution

$$(3.2a) \quad z(t) = \int_{-\infty}^t \alpha(t-s) \odot r(s) \, ds,$$

$$(3.2b) \quad r(t) = h(x(t)),$$

where $r : \mathbb{R} \rightarrow \mathbb{R}^{n_z}$ is the delayed variable, and each element of $\alpha : \mathbb{R}_{\geq 0} \rightarrow \mathbb{R}^{n_z}$ is an exponentially bounded *regular* kernel (see Definition 3.2–3.3). Furthermore, $h : \mathbb{R}^{n_x} \rightarrow \mathbb{R}^{n_z}$ is the memory function. We assume that f and h are differentiable in their arguments and that r is bounded, i.e., that $\|r(t)\|_{\infty} \leq K_r$ for all $t \in (-\infty, t_f]$. Additionally, we assume that x_0 is continuous and exponentially bounded, i.e., $\|x_0(t)\|_{\infty} \leq L_0 e^{-\sigma t}$, and that the rate parameter, $\sigma \in \mathbb{R}_{>0}$, is strictly smaller than all of the rate parameters in the exponential bounds for the kernels. We refer to the paper by Ponosov et al. [40, Thm. 1] for more details on the existence and uniqueness of solutions to the initial value problem (IVP) (3.1)–(3.2). See also the book by Hale and Lunel [20].

Definition 3.1. For a scalar-valued kernel, $\alpha : \mathbb{R}_{\geq 0} \rightarrow \mathbb{R}$, the integrals $\beta : \mathbb{R}_{\geq 0} \rightarrow \mathbb{R}$ and $\rho : \mathbb{R}_{\geq 0} \rightarrow \mathbb{R}_{\geq 0}$ are defined by

$$(3.3) \quad \beta(t) = \int_0^t \alpha(s) \, ds, \quad \rho(t) = \int_0^t |\alpha(s)| \, ds.$$

Definition 3.2. A scalar-valued kernel, $\alpha : \mathbb{R}_{\geq 0} \rightarrow \mathbb{R}$, is regular if it satisfies the following conditions.

- (a) It is bounded, i.e., $|\alpha(t)| \leq K$ for all $t \in \mathbb{R}_{\geq 0}$ and for some finite $K \in \mathbb{R}_{>0}$.
- (b) It is continuous, i.e., for all $\epsilon \in \mathbb{R}_{>0}$ and $t \in \mathbb{R}_{\geq 0}$, there exists a $\delta \in \mathbb{R}_{>0}$ such that $|\alpha(s) - \alpha(t)| < \epsilon$ for all $s \in \mathbb{R}_{\geq 0}$ satisfying $|s - t| < \delta$.
- (c) The integral of the absolute value of α is finite:

$$(3.4) \quad \rho(\infty) = \int_0^{\infty} |\alpha(s)| \, ds < \infty.$$

Definition 3.3. A scalar-valued kernel, $\alpha : \mathbb{R}_{\geq 0} \rightarrow \mathbb{R}$, is exponentially bounded if there exist $L, \rho \in \mathbb{R}_{>0}$ such that

$$(3.5) \quad |\alpha(t)| \leq L e^{-\rho t}$$

for all $t \in \mathbb{R}_{\geq 0}$.

Next, we present a few corollaries from the literature about the steady states of (3.1b)–(3.2) and their stability.

Corollary 3.4. *A state $\bar{x} \in \mathbb{R}^{n_x}$ is a steady state of the system (3.1b)–(3.2) if*

$$(3.6) \quad 0 = f(\bar{x}, \bar{z}), \quad \bar{z} = \beta(\infty) \odot \bar{r}, \quad r(t) = h(\bar{x})m$$

where the i 'th element of $\beta : \mathbb{R}_{\geq 0} \rightarrow \mathbb{R}^{n_z}$ is given by (3.3) in Definition 3.1.

Proof. In steady state, $x(t) = \bar{x}$ for all t . Consequently, $r(t) = \bar{r} = h(\bar{x})$ and

$$(3.7) \quad z(t) = \int_{-\infty}^t \alpha(t-s) \odot \bar{r} ds = \int_{-\infty}^t \alpha(t-s) ds \odot \bar{r} = \beta(\infty) \odot \bar{r},$$

for all t . ■

Corollary 3.5. *The linearization of the system (3.1b)–(3.2) around a steady state, \bar{x} , satisfying (3.6) describes the evolution of the deviation variable $X : \mathbb{R} \rightarrow \mathbb{R}^{n_x}$:*

$$(3.8) \quad \dot{X}(t) = FX(t) + G \int_{-\infty}^t \alpha(t-s) \odot HX(s) ds, \quad X(t) = x(t) - \bar{x}.$$

The matrices $F \in \mathbb{R}^{n_x \times n_x}$, $G \in \mathbb{R}^{n_x \times n_z}$, and $H \in \mathbb{R}^{n_z \times n_x}$ are the Jacobians of the right-hand side function and the delay function evaluated in the steady state:

$$(3.9) \quad F = \frac{\partial f}{\partial x}(\bar{x}, \bar{z}), \quad G = \frac{\partial f}{\partial z}(\bar{x}, \bar{z}), \quad H = \frac{\partial h}{\partial x}(\bar{x}).$$

Corollary 3.6. *The system (3.1b)–(3.2) is locally asymptotically stable around a steady state, \bar{x} , satisfying (3.6) if $\text{Re } \lambda < 0$ for all $\lambda \in \mathbb{C}$ that satisfy the characteristic equation*

$$(3.10) \quad P(\lambda) = \det \left(F - \lambda I + G \int_0^{\infty} e^{-\lambda s} \text{diag } \alpha(s) ds H \right) = 0,$$

where $P : \mathbb{C} \rightarrow \mathbb{C}$ is the characteristic function and $I \in \mathbb{R}^{n_x \times n_x}$ is an identity matrix.

Proof. Theorem 4.7 in the paper by Diekmann and Gyllenberg [11] provides conditions under which this result holds, and the assumptions on the system (3.1b)–(3.2) ensure that these conditions are satisfied (see Section SM1 in the supplementary material for further details). ■

4. Main theoretical results. In this section, we present and prove the two main theoretical results of the paper: 1) We can approximate regular kernels arbitrarily well using Erlang mixture approximations (Proposition 4.2), and 2) we can approximate the DDEs (3.1b)–(3.2) by ODEs based on Erlang mixture approximations because of convergence results for the solution and steady state of the ODEs and for the roots of the characteristic polynomial as well as a result on the stability of the error of the solution (Theorem 4.4). For simplicity of the presentation, we only consider scalar kernels in Proposition 4.2 on the convergence of Erlang mixture approximations.

First, we define Erlang kernels which constitute the basis functions in the Erlang mixture kernel approximation that we describe afterwards. Figure 1 shows examples of Erlang kernels and Erlang mixture kernels for different rate parameters and coefficients.

Definition 4.1. The m 'th order Erlang kernel, $\ell_m : \mathbb{R}_{\geq 0} \rightarrow \mathbb{R}_{\geq 0}$, with rate parameter $a \in \mathbb{R}_{> 0}$ is given by [28]

$$(4.1) \quad \ell_m(t) = b_m t^m e^{-at}, \quad b_m = \frac{a^{m+1}}{m!},$$

where $b_m \in \mathbb{R}_{\geq 0}$ is a normalization constant, and $m \in \mathbb{N}_{\geq 0}$.

The normalization constant, b_m , is defined such that the integral of the Erlang kernel is one:

$$(4.2) \quad \int_0^\infty \ell_m(t) dt = 1.$$

Proposition 4.2 (Erlang mixture approximation). Let $\alpha : \mathbb{R}_{\geq 0} \rightarrow \mathbb{R}$ be a scalar-valued regular kernel, and let $\hat{\alpha} : \mathbb{R}_{\geq 0} \rightarrow \mathbb{R}$ be an Erlang mixture kernel of order $M \in \mathbb{N}_{\geq 0}$ and rate parameter $a \in \mathbb{R}_{> 0}$ defined by

$$(4.3) \quad \hat{\alpha}(t) = \sum_{m=0}^M c_m \ell_m(t), \quad c_m = \int_{s_m}^{s_{m+1}} \alpha(s) ds, \quad s_m = m\Delta s, \quad \Delta s = 1/a,$$

where $c_m \in \mathbb{R}$ is the m 'th coefficient given by the integral of α over a set of intervals with boundaries $s_m \in \mathbb{R}_{\geq 0}$ for $m = 0, \dots, M+1$ where the width $\Delta s \in \mathbb{R}_{> 0}$ is equal to the inverse of the rate parameter, a . Then,

(a) $\hat{\alpha}$ is regular,

and the following asymptotic properties hold as $a \rightarrow \infty$ provided that $M/a \rightarrow \infty$ as well.

(b) $\hat{\alpha}$ converges uniformly to α for all $t \in \mathbb{R}_{\geq 0}$, i.e.,

$$(4.4) \quad \hat{\alpha}(t) \rightarrow \alpha(t).$$

(c) $\hat{\alpha}$ converges weakly to α for all $t \in \mathbb{R}_{\geq 0}$, i.e.,

$$(4.5) \quad \int_0^t \hat{\alpha}(s) ds \rightarrow \int_0^t \alpha(s) ds.$$

(d) The integral of the absolute difference between $\hat{\alpha}$ and α converges to zero:

$$(4.6) \quad \int_0^\infty |\hat{\alpha}(t) - \alpha(t)| dt \rightarrow 0.$$

Corollary 4.3. The Erlang mixture kernel, $\hat{\alpha}$, defined in Proposition 4.2 is exponentially bounded if α is exponentially bounded. Specifically, if $|\alpha(t)| \leq L e^{-\rho t}$ for all $t \in \mathbb{R}_{\geq 0}$ where $L, \rho \in \mathbb{R}_{> 0}$, then $|\hat{\alpha}(t)| \leq L e^{-\bar{\rho} t}$ where $\bar{\rho} = \rho(1 - e^{-\omega})/\omega \in \mathbb{R}_{> 0}$. Furthermore, $0 \leq \bar{\rho} < \rho$ and $\bar{\rho} \rightarrow \rho$ as $\omega \rightarrow 0$.

Theorem 4.4 (ODE approximation). Consider the system of DDEs (3.1b)–(3.2), and let $\hat{\alpha}_i : \mathbb{R} \rightarrow \mathbb{R}_{\geq 0}$ be the Erlang mixture approximation of the i 'th kernel, α_i , of order $M_i \in \mathbb{N}_{\geq 0}$

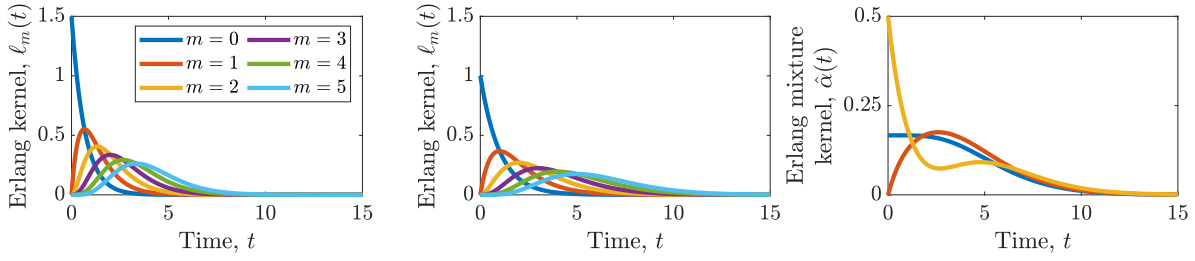


Figure 1. Erlang kernels for $a = 1.5$ (left) and $a = 1$ (middle) and $m = 0, \dots, 5$, and an Erlang mixture kernel (right) for $a = 1$, $M = 5$, and the following values of the coefficients. Blue: $c_m = 1/(M + 1)$ for $m = 0, \dots, M$. Red: $c_0 = 0$ and $c_m = 1/M$ for $m = 1, \dots, M$. Yellow: $c_0 = c_M = 1/2$ and $c_m = 0$ for $m = 1, \dots, M - 1$.

with rate parameter $a_i \in \mathbb{R}_{>0}$ (see Proposition 4.2). Furthermore, consider the system of ODEs

$$(4.7a) \quad \dot{\hat{x}}(t) = f(\hat{x}(t), \hat{z}(t)),$$

$$(4.7b) \quad \dot{\hat{Z}}(t) = A\hat{Z}(t) + B\hat{r}(t),$$

$$(4.7c) \quad \hat{z}(t) = C\hat{Z}(t),$$

$$(4.7d) \quad \hat{r}(t) = h(\hat{x}(t)),$$

where $\hat{x} : \mathbb{R} \rightarrow \mathbb{R}^{n_x}$, $\hat{z}, \hat{r} : \mathbb{R} \rightarrow \mathbb{R}^{n_z}$, and $\hat{Z} : \mathbb{R} \rightarrow \mathbb{R}^{M+n_z}$. Here, $M = \sum_{i=1}^{n_z} M_i$, and the elements of \hat{Z} are the auxiliary memory states $\hat{z}_{mi} : \mathbb{R} \rightarrow \mathbb{R}$ for $m = 0, \dots, M_i$ and $i = 1, \dots, n_z$ ordered as $\hat{Z} = [\hat{z}_{00} \ \hat{z}_{10} \ \cdots \ \hat{z}_{M_{n_z}, n_z}]^T$, and the initial conditions are

$$(4.8a) \quad \hat{x}(t) = x_0(t), \quad t \in (-\infty, t_0],$$

$$(4.8b) \quad z_{mi}(t_0) = \int_{-\infty}^{t_0} \ell_{mi}(t_0 - s) \hat{r}_i(s) ds, \quad m = 0, \dots, M_i, \quad i = 1, \dots, n_z,$$

where x_0 is the initial state function in (3.1a). The matrices $A \in \mathbb{R}^{M+n_z \times M+n_z}$, $B \in \mathbb{R}_{\geq 0}^{M+n_z \times n_z}$, and $C \in \mathbb{R}^{n_z \times M+n_z}$ are block-diagonal:

$$(4.9a) \quad A = \text{blkdiag} \left(A^{(1)}, A^{(2)}, \dots, A^{(n_z)} \right),$$

$$(4.9b) \quad B = \text{blkdiag} \left(b^{(1)}, b^{(2)}, \dots, b^{(n_z)} \right),$$

$$(4.9c) \quad C = \text{blkdiag} \left(c^{(1)}, c^{(2)}, \dots, c^{(n_z)} \right).$$

The block-diagonal elements, $A^{(i)} \in \mathbb{R}^{(M_i+1) \times (M_i+1)}$, $b^{(i)} \in \mathbb{R}_{\geq 0}^{M_i+1 \times 1}$, and $c^{(i)} \in \mathbb{R}^{1 \times M_i+1}$, are given by

$$(4.10) \quad A^{(i)} = a_i(L^{(i)} - I^{(i)}), \quad b^{(i)} = a_i e_1^{(i)}, \quad c^{(i)} = [c_{0,i} \ c_{1,i} \ \cdots \ c_{M_i,i}], \quad i = 1, \dots, n_z,$$

where $I^{(i)}, L^{(i)} \in \mathbb{R}^{M_i+1 \times M_i+1}$ are an identity matrix and a lower shift matrix, respectively, i.e., $L^{(i)}$ contains ones in the first subdiagonal and zeros elsewhere. Furthermore, the first

element of $e_1^{(i)} \in \mathbb{R}^{M_i+1 \times 1}$ is one and the others are zero, and $c_{m,i} \in \mathbb{R}$ is the m 'th coefficient in the i 'th Erlang mixture approximation. Then, the following asymptotic properties hold as $a_i \rightarrow \infty$ provided that $M_i/a_i \rightarrow \infty$ as well for $i = 1, \dots, n_z$.

- (a) The steady state of the ODEs (4.7) converges to that of the DDEs (3.1b)–(3.2) if the matrix $F + G \operatorname{diag} \beta(\infty) H$ is invertible, where F , G , and H are given by (3.9).
- (b) For every isolated root, $\lambda \in \mathbb{C}$, of the characteristic function in (3.10), there are roots of the characteristic function for the ODEs (4.7) that converge to λ provided that $\operatorname{Re} \lambda \geq \lambda_{\min}$ where $-\rho_i < \lambda_{\min} \in \mathbb{R}_{\leq 0}$ for $i = 1, \dots, n_z$. The i 'th rate parameter, $\rho_i \in \mathbb{R}_{> 0}$, is obtained from the exponential bound on α_i (see Definition 3.3).
- (c) If the DDEs (3.1b)–(3.2) and ODEs (4.7) are locally asymptotically stable around their respective steady states, so is the dynamical system describing the state error, $x - \hat{x}$.
- (d) The solution, \hat{x} , to the IVP (4.7)–(4.8) involving ODEs, the memory state \hat{z} , and the delayed quantity \hat{r} converge uniformly to the solution, x , to the IVP (3.1)–(3.2) involving DDEs, the memory state z , and the delayed quantity r , respectively, for $t \in (-\infty, t_f]$.

Corollary 4.5. *If the initial state function, x_0 , is constant, then $\hat{z}_{mi}(t_0) = \hat{r}_{i,0}$ where $\hat{r}_0 = h(x_0)$.*

Proof. The result follows from the fact that, by definition, the Erlang kernels in (4.1) integrate to one:

$$(4.11) \quad \hat{z}_{mi}(t_0) = \int_{-\infty}^{t_0} \ell_{mi}(t_0 - s) \hat{r}_i(s) ds = \hat{r}_{i,0} \int_{-\infty}^{t_0} \ell_{mi}(t_0 - s) ds = \hat{r}_{i,0}. \quad \blacksquare$$

In the remainder of this section, we present proofs of the statements in Proposition 4.2 and Theorem 4.4.

4.1. Regularity and convergence of Erlang mixture approximations. In this section, we prove that the Erlang mixture approximation defined in Proposition 4.2 is regular, that it converges uniformly and weakly (i.e., the integral converges), and that the integral of the absolute error converges to zero as the rate parameter, a , goes to infinity provided that the ratio M/a also goes to infinity, i.e., that the order, M , approaches infinity faster than a .

Proof of Proposition 4.2(a). The boundedness in Definition 3.2(a) follows directly from the substitution of the upper bound on α into the expression for the coefficients in (4.3):

$$(4.12) \quad |\hat{\alpha}(t)| = \left| \sum_{m=0}^M \ell_m(t) \int_{s_m}^{s_{m+1}} \alpha(s) ds \right| \leq \sum_{m=0}^M \ell_m(t) \int_{s_m}^{s_{m+1}} K ds = K \sum_{m=0}^M \ell_m(t) \Delta s \\ = K \sum_{m=0}^M \frac{(at)^m}{m!} a e^{-at} \frac{1}{a} = K \sum_{m=0}^M \frac{(at)^m}{m!} e^{-at} \leq K e^{at} e^{-at} = K,$$

where we have used the identity (2.2) and that all terms in the sum are positive, i.e., $\sum_{m=0}^M (at)^m/m! \leq \sum_{m=0}^{\infty} (at)^m/m! = e^{at}$ for all $a \in \mathbb{R}_{> 0}$ and $M \in \mathbb{N}_{\geq 0}$. The continuity of $\hat{\alpha}$ in Definition 3.2(b) follows directly from the fact that it is a weighted sum of the Erlang kernels, ℓ_m , which are continuous because they are products of monomials and exponential

functions. Finally, we show that the integral of the absolute value of $\hat{\alpha}$ is finite as in Definition 3.2(c):

$$(4.13) \quad \begin{aligned} \int_0^\infty |\hat{\alpha}(s)| ds &= \int_0^\infty \left| \sum_{m=0}^M c_m \ell_m(s) \right| ds \leq \sum_{m=0}^M |c_m| \int_0^\infty \ell_m(s) ds = \sum_{m=0}^M |c_m| \\ &= \sum_{m=0}^M \left| \int_{s_m}^{s_{m+1}} \alpha(s) ds \right| \leq \int_0^{s_{M+1}} |\alpha(s)| ds \leq \int_0^\infty |\alpha(s)| ds = \rho(\infty) < \infty. \end{aligned}$$

Here, we have used Minkowski's inequality and that the Erlang kernels are non-negative and integrate to one. \blacksquare

Proof of Proposition 4.2(b). In order to prove that the Erlang mixture approximation $\hat{\alpha}$ converges uniformly to α , we express it in terms of the delta family, $\delta_a : \mathbb{R}_{\geq 0} \times \mathbb{R}_{\geq 0} \rightarrow \mathbb{R}_{\geq 0}$, defined by (B.1) in Lemma B.1:

$$(4.14) \quad \hat{\alpha}(t) = \int_0^\infty \delta_a(t, s) \alpha(s) ds.$$

This equality holds according to Lemma B.1(a), and since δ_a satisfies Lemma B.1(b)–(d), Lemma D.1 guarantees that $\hat{\alpha}$ converges uniformly to α for all $t \in \mathbb{R}_{\geq 0}$. \blacksquare

Proof of Proposition 4.2(c). First, we bound the absolute difference between the two integrals:

$$(4.15) \quad \left| \int_0^t \hat{\alpha}(s) ds - \int_0^t \alpha(s) ds \right| \leq \int_0^t |\hat{\alpha}(s) - \alpha(s)| ds \leq t \sup_{s \in [0, t]} |\hat{\alpha}(s) - \alpha(s)|.$$

For finite t , the rightmost expression goes to zero as $a \rightarrow \infty$ and $M/a \rightarrow \infty$. When t is infinite, we split the integral at $t_0 \in \mathbb{R}_{\geq 0}$:

$$(4.16) \quad \left| \int_0^\infty \hat{\alpha}(s) ds - \int_0^\infty \alpha(s) ds \right| \leq \int_0^{t_0} |\hat{\alpha}(s) - \alpha(s)| ds + \int_{t_0}^\infty |\hat{\alpha}(s) - \alpha(s)| ds.$$

As α is regular, the integral of its absolute value is finite. Furthermore, according to Lemma E.2, $\hat{\alpha}$ is tight, i.e., we can choose t_0 large enough that the second term is below $\epsilon/2$ for all values of a and M . Next, we choose a and M large enough that the first term is below $\epsilon/2$ as well, which concludes the proof. \blacksquare

Proof of Proposition 4.2(d). As α is regular, it is bounded. According to Proposition 4.2(a), this means that $\hat{\alpha}$ is also bounded because it is also regular. Consequently, according to Lemma E.1, $\hat{\alpha}$ is uniformly integrable. Furthermore, according to Lemma E.2 and Proposition 4.2(b), $\hat{\alpha}$ is also tight and converges pointwise to α (because it converges uniformly). Finally, according to Vitali's convergence lemma [47, Sec. 19.1, p. 399], uniform integrability, tightness, and pointwise convergence implies that $\hat{\alpha}$ also converges in the L^1 -norm, i.e., the stated result. \blacksquare

4.2. Steady states and stability criteria. In this section, we show that the steady state of the approximate system of ODEs converges to that of the original system, and we present the steady state stability criterion. In Section 4.3, we show that the roots involved in the criterion converge to those in the criterion for the original system of DDEs.

Lemma 4.6. *A steady state, $\bar{x} \in \mathbb{R}^{n_x}$, of the approximate system of ODEs (4.7) satisfies*

$$(4.17) \quad 0 = f(\bar{x}, \bar{z}), \quad \bar{z} = d \odot \bar{r}, \quad \bar{r} = h(\bar{x}),$$

where $d \in \mathbb{R}^{n_z}$ and $d_i = \sum_{m=0}^{M_i} c_{m,i}$ for $i = 1, \dots, n_z$.

Proof. In steady state,

$$(4.18) \quad 0 = f(\bar{x}, \bar{z}), \quad 0 = A\bar{Z} + B\bar{r}.$$

Consequently,

$$(4.19) \quad \bar{Z} = -A^{-1}B\bar{r}, \quad \bar{z} = C\bar{Z} = -CA^{-1}B\bar{r}.$$

Note that each block-diagonal element of A is a lower bidiagonal matrix with nonzero elements in the diagonal and the first subdiagonal. Therefore, A is invertible. Specifically,

$$(4.20a) \quad A^{-1} = \text{blkdiag} \left(\left(A^{(1)} \right)^{-1}, \dots, \left(A^{(n_z)} \right)^{-1} \right),$$

$$(4.20b) \quad CA^{-1}B = \text{diag} \left(c^{(1)} \left(A^{(1)} \right)^{-1} b^{(1)}, \dots, c^{(n_z)} \left(A^{(n_z)} \right)^{-1} b^{(n_z)} \right).$$

The inverse of $A^{(i)}$ is a multiple of a lower triangular matrix of ones and the diagonal elements of (4.20b) can be derived analytically:

$$(4.21) \quad \left(A^{(i)} \right)^{-1} = \frac{-1}{a_i} \begin{bmatrix} 1 & & & \\ 1 & 1 & & \\ \vdots & & \ddots & \\ 1 & 1 & \cdots & 1 \end{bmatrix}, \quad c^{(i)} \left(A^{(i)} \right)^{-1} b^{(i)} = - \sum_{m=0}^{M_i} c_{m,i}.$$

Consequently, $-CA^{-1}B = \text{diag } d$, and

$$(4.22) \quad \bar{z} = d \odot \bar{r}, \quad \bar{r} = h(\bar{x}). \quad \blacksquare$$

Proof of Theorem 4.4(a). First, according to Proposition 4.2(c),

$$(4.23) \quad d_i = \sum_{m=0}^{M_i} c_{m,i} = \int_0^\infty \hat{\alpha}_i(s) ds \rightarrow \beta_i(\infty)$$

as $a_i \rightarrow \infty$ when $M_i/a_i \rightarrow \infty$ as well. Next, the implicit function theorem [41, Chap. 7, Thm. 3] guarantees that the solution to the steady state equations (3.6) for the DDEs (3.1b)–(3.2) is a locally unique and differentiable function if the Jacobian with respect to \bar{x} is invertible.

Consequently, in that case, the solution to the steady state equations (4.17) for the ODEs (4.7) converges to that of the DDEs (3.1b)–(3.2). Furthermore, the Jacobian is given by

$$(4.24) \quad \frac{df}{d\bar{x}}(\bar{x}, \bar{z}) = \frac{\partial f}{\partial x}(\bar{x}, \bar{z}) + \frac{\partial f}{\partial z}(\bar{x}, \bar{z}) \frac{\partial \bar{z}}{\partial \bar{x}}, \quad \frac{\partial \bar{z}}{\partial \bar{x}} = \text{diag } \beta(\infty) \frac{\partial \bar{r}}{\partial \bar{x}}, \quad \frac{\partial \bar{r}}{\partial \bar{x}} = \frac{\partial h}{\partial x}(\bar{x}),$$

and the matrix in Theorem 4.4(a) is obtained by substituting the matrices F , G , and H from (3.9). \blacksquare

Lemma 4.7. *The system of approximate ODEs (4.7) is locally asymptotically stable around a steady state, \bar{x} , that satisfies (4.17) if $\text{Re } \lambda < 0$ for all eigenvalues $\lambda \in \mathbb{C}$ of the Jacobian matrix*

$$(4.25) \quad J = \begin{bmatrix} \hat{F} & \hat{G}C \\ B\hat{H} & A \end{bmatrix},$$

where $\hat{F} \in \mathbb{R}^{n_x \times n_x}$, $\hat{G} \in \mathbb{R}^{n_x \times n_z}$, and $\hat{H} \in \mathbb{R}^{n_z \times n_x}$ are the Jacobian matrices (3.9) evaluated in the steady state for the approximate system. Furthermore, the eigenvalues, λ , that are not equal to $-a_i$ for $i = 1, \dots, n_z$ will also satisfy the reduced characteristic equation

$$(4.26) \quad \hat{P}(\lambda) = \det(\hat{F} - \lambda I + \hat{G}Q(\lambda)\hat{H}) = 0, \quad Q_{ij}(\lambda) = \begin{cases} \sum_{m=0}^{M_i} c_{m,i} \left(\frac{a_i}{a_i + \lambda}\right)^{m+1}, & i = j, \\ 0, & i \neq j, \end{cases}$$

where $\hat{P} : \mathbb{C} \rightarrow \mathbb{C}$ is the approximate characteristic function and $Q : \mathbb{C} \rightarrow \mathbb{C}^{n_z \times n_x}$ is an auxiliary matrix.

Proof. An eigenvalue, λ , is a root of the characteristic polynomial

$$(4.27) \quad \det(J - \lambda I) = \det \begin{bmatrix} \hat{F} - \lambda I & \hat{G}C \\ B\hat{H} & A - \lambda I \end{bmatrix} \\ = \det \left(\hat{F} - \lambda I - \hat{G}C(A - \lambda I)^{-1}B\hat{H} \right) \det(A - \lambda I),$$

where we have used Schur's determinant formula (see, e.g., [56]), which presumes that $\det(A - \lambda I) \neq 0$. Next, we exploit the block-diagonal structure of A :

$$(4.28) \quad A - \lambda I = \text{blkdiag} \left(A^{(1)} - \lambda I^{(1)}, \dots, A^{(n_z)} - \lambda I^{(n_z)} \right).$$

Consequently,

$$(4.29) \quad \det(A - \lambda I) = \prod_{i=1}^{n_z} \det(A^{(i)} - \lambda I^{(i)}) = \prod_{i=1}^{n_z} (-1)^{M_i} (a_i + \lambda)^{M_i},$$

which is nonzero by assumption such that $A - \lambda I$ is invertible. Next, we consider the diagonal matrix

$$(4.30) \quad C(A - \lambda I)^{-1}B = \text{diag} \left(c^{(1)} \left(A^{(1)} - \lambda I^{(1)} \right)^{-1} b^{(1)}, \dots, c^{(n_z)} \left(A^{(n_z)} - \lambda I^{(n_z)} \right)^{-1} b^{(n_z)} \right).$$

First, we rewrite the matrix

$$(4.31) \quad A^{(i)} - \lambda I^{(i)} = a_i \left(L^{(i)} - I^{(i)} \right) - \lambda I^{(i)} = -(a_i + \lambda) \left(\frac{-a_i}{a_i + \lambda} L^{(i)} + I^{(i)} \right).$$

Consequently, the inverse is

$$(4.32) \quad \left(A^{(i)} - \lambda I^{(i)} \right)^{-1} = \frac{-1}{a_i + \lambda} \begin{bmatrix} 1 & & & \\ \frac{a_i}{a_i + \lambda} & 1 & & \\ \vdots & & \ddots & \\ \left(\frac{a_i}{a_i + \lambda} \right)^{M_i} & \left(\frac{a_i}{a_i + \lambda} \right)^{M_i - 1} & \cdots & 1 \end{bmatrix},$$

as can be verified by direct calculation, and the diagonal elements of the matrix in (4.30) are

$$(4.33) \quad c^{(i)} \left(A^{(i)} - \lambda I^{(i)} \right)^{-1} b^{(i)} = - \sum_{m=0}^{M_i} c_{m,i} \left(\frac{a_i}{a_i + \lambda} \right)^{m+1} = -Q_{ii}(\lambda).$$

Finally, we substitute into the left determinant on the right-hand side of (4.27) and obtain

$$(4.34) \quad \det(\hat{F} - \lambda I + \hat{G}Q(\lambda)\hat{H}) = 0. \quad \blacksquare$$

Corollary 4.8. *Let each element of $\hat{\alpha} : \mathbb{R}_{\geq 0} \rightarrow \mathbb{R}^{n_z}$ be an Erlang mixture kernel. Then, the approximate characteristic function $\hat{P} : \mathbb{C} \rightarrow \mathbb{C}$ and the auxiliary matrix $Q : \mathbb{C} \rightarrow \mathbb{C}^{n_z \times n_z}$ defined in (4.26) in Lemma 4.7 are equal to*

$$(4.35) \quad \hat{P}(\lambda) = \det(\hat{F} - \lambda I + \hat{G} \int_0^\infty e^{-\lambda s} \text{diag } \hat{\alpha}(s) \, ds \hat{H}), \quad Q_{ii}(\lambda) = \int_0^\infty e^{-\lambda s} \hat{\alpha}_i(s) \, ds,$$

for $i = 1, \dots, n_z$.

Proof. The result follows directly from the equivalence of the approximate systems of DDEs (F.1) and ODEs (4.7) and the stability criterion in Corollary 3.6. However, for completeness, we write out the proof in detail. First, we write out the following integral for an Erlang kernel of order m with rate parameter a_i :

$$(4.36) \quad \int_0^\infty e^{-\lambda s} \ell_{m,i}(s) \, ds = b_{m,i} \int_0^\infty s^m e^{-(a_i + \lambda)s} \, ds = b_{m,i} \frac{m!}{(a_i + \lambda)^{m+1}} = \left(\frac{a_i}{a_i + \lambda} \right)^{m+1}.$$

This follows from the fact that the integral of an Erlang kernel of order m with rate parameter $a_i + \lambda$ is one. Next, we use this result to write out the following integral involving an Erlang mixture kernel of order M_i with rate parameter a_i :

$$(4.37) \quad \int_0^\infty e^{-\lambda s} \hat{\alpha}_i(s) \, ds = \sum_{m=0}^{M_i} c_{m,i} \int_0^\infty e^{-\lambda s} \ell_{m,i}(s) \, ds = \sum_{m=0}^{M_i} c_{m,i} \left(\frac{a_i}{a_i + \lambda} \right)^{m+1} = Q_{ii}(\lambda).$$

Consequently,

$$(4.38) \quad \hat{G} \int_0^\infty e^{-\lambda s} \text{diag } \hat{\alpha}(s) \, ds \hat{H} = \hat{G} \text{diag} \left\{ \int_0^\infty e^{-\lambda s} \hat{\alpha}_i(s) \, ds \right\}_{i=1}^{n_z} \hat{H} = \hat{G}Q(\lambda)\hat{H},$$

and the characteristic function in (3.10) becomes

$$(4.39) \quad \hat{P}(\lambda) = \det(\hat{F} - \lambda I + \hat{G}Q(\lambda)\hat{H}). \quad \blacksquare$$

4.3. Convergence of the roots. In this section, we use Hurwitz' convergence theorem [19, Thm. 5.6.4] to prove that the roots of the approximate characteristic function, $\hat{P} : \mathbb{C} \rightarrow \mathbb{C}$ in Lemma 4.7, converge to the isolated roots of $P : \mathbb{C} \rightarrow \mathbb{C}$ in Corollary 3.6 as the rate parameters and order in the Erlang mixture approximation go to infinity. That is, we show that stability analyses based on the approximate system of ODEs in (4.7) can be used to partially infer information about the stability of the original DDEs.

Lemma 4.9. *Let each element of $\alpha : \mathbb{R}_{\geq 0} \rightarrow \mathbb{R}^{n_z}$ be a regular and exponentially bounded kernel, i.e., let there exist $L, \rho \in \mathbb{R}_{> 0}$ such that $|\alpha_i(t)| \leq Le^{-\rho t}$ for all $t \in \mathbb{R}_{\geq 0}$ and for $i = 1, \dots, n_z$. Furthermore, let the i 'th element of $\hat{\alpha} : \mathbb{R}_{\geq 0} \rightarrow \mathbb{R}^{n_z}$ be the Erlang mixture approximation of α_i of order $M_i \in \mathbb{N}_{\geq 0}$ with rate parameter $a_i \in \mathbb{R}_{> 0}$. Then, for a given $\lambda_{\min} \in \mathbb{R}_{\leq 0}$ for which $-\rho < \lambda_{\min}$, the approximate characteristic function $\hat{P} : \mathbb{C} \rightarrow \mathbb{C}$ defined in (4.26) converges uniformly to the characteristic function $P : \mathbb{C} \rightarrow \mathbb{C}$ defined in (3.10) for every $\lambda \in \mathbb{C}$ for which $\text{Re } \lambda \geq \lambda_{\min}$ as $a_i \rightarrow \infty$ if $M_i/a_i \rightarrow \infty$ as well for $i = 1, \dots, n_z$.*

Proof. Both \hat{P} and P are determinants of characteristic matrices. Consequently, since the determinant is continuous, \hat{P} converges to P if the corresponding characteristic matrix converges. First, we bound the following expression and split the integral,

$$(4.40) \quad \left| Q_{ii}(\lambda) - \int_0^\infty e^{-\lambda s} \alpha_i(s) ds \right| = \left| \int_0^\infty e^{-\lambda s} \hat{\alpha}_i(s) ds - \int_0^\infty e^{-\lambda s} \alpha_i(s) ds \right| \\ \leq \int_0^\infty |e^{-\lambda s}| |\hat{\alpha}_i(s) - \alpha_i(s)| ds = \int_0^{s_0} e^{-\text{Re } \lambda s} |\hat{\alpha}_i(s) - \alpha_i(s)| ds + \int_{s_0}^\infty e^{-\text{Re } \lambda s} |\hat{\alpha}_i(s) - \alpha_i(s)| ds.$$

Here, we have used the expression for Q_{ii} from Corollary 4.8. We consider the second integral first. The exponential boundedness of α implies that $\hat{\alpha}$ is also exponentially bounded (see Corollary 4.3) such that

$$(4.41) \quad \int_{s_0}^\infty e^{-\text{Re } \lambda s} |\hat{\alpha}_i(s) - \alpha_i(s)| ds \leq \int_{s_0}^\infty e^{-\lambda_{\min} s} 2L e^{-\bar{\rho} s} ds = 2L \int_{s_0}^\infty e^{-(\lambda_{\min} + \bar{\rho}) s} ds \\ = \frac{2L}{\lambda_{\min} + \bar{\rho}} e^{-(\lambda_{\min} + \bar{\rho}) s_0}.$$

By assumption, $\lambda_{\min} > -\rho$, and according to Corollary 4.3, we can always choose $\bar{a} \in \mathbb{R}_{> 0}$ and $\bar{M} \in \mathbb{N}_{\geq 0}$ (for which $\bar{M}/\bar{a} \rightarrow \infty$ as $\bar{a} \rightarrow \infty$) such that $\bar{\rho}$ is arbitrarily close to ρ for all $a_i > \bar{a}$ and $M_i > \bar{M}$, i.e., such that $\lambda_{\min} + \bar{\rho} > 0$. Next, we bound the first integral, and we exploit the non-positivity of λ_{\min} :

$$(4.42) \quad \int_0^{s_0} e^{-\text{Re } \lambda s} |\hat{\alpha}_i(s) - \alpha_i(s)| ds \leq \int_0^{s_0} e^{-\lambda_{\min} s} |\hat{\alpha}_i(s) - \alpha_i(s)| ds \\ \leq e^{-\lambda_{\min} s_0} \int_0^{s_0} |\hat{\alpha}_i(s) - \alpha_i(s)| ds.$$

According to Proposition 4.2(d) and because the integrand is non-negative, we can choose \bar{a} and \bar{M} (for which $\bar{M}/\bar{a} \rightarrow \infty$ as $\bar{a} \rightarrow \infty$) large enough that the last integral is arbitrarily small for $a_i > \bar{a}$ and $M_i > \bar{M}$. Finally, we bound the norm difference between the characteristic

matrices in the expressions for \hat{P} and P in (4.35) and (3.10), respectively, and we use the ∞ -norm for convenience:

$$\begin{aligned}
(4.43) \quad & \left\| \hat{F} - \lambda I + \hat{G} \int_0^\infty e^{-\lambda s} \text{diag } \hat{\alpha}(s) \, ds \hat{H} - \left(F - \lambda I + G \int_0^\infty e^{-\lambda s} \text{diag } \alpha(s) \, ds H \right) \right\|_\infty \\
&= \left\| \hat{F} - F + \hat{G} \int_0^\infty e^{-\lambda s} \text{diag } \hat{\alpha}(s) \, ds (\hat{H} - H) \right. \\
&\quad \left. + \hat{G} \int_0^\infty e^{-\lambda s} \text{diag}(\hat{\alpha}(s) - \alpha(s)) \, ds H + (\hat{G} - G) \int_0^\infty e^{-\lambda s} \text{diag } \alpha(s) \, ds H \right\|_\infty \\
&\leq \|e_F\|_\infty + \|\hat{G}\|_\infty \int_0^\infty |e^{-\lambda s}| \|\text{diag } \hat{\alpha}(s)\|_\infty \, ds \|e_H\|_\infty \\
&\quad + \|\hat{G}\|_\infty \left\| \int_0^\infty e^{-\lambda s} \text{diag}(\hat{\alpha}(s) - \alpha(s)) \, ds \right\|_\infty \|H\|_\infty + \|e_G\|_\infty \int_0^\infty |e^{-\lambda s}| \|\text{diag } \alpha(s)\|_\infty \, ds \|H\|_\infty
\end{aligned}$$

Here, $e_F = \hat{F} - F \in \mathbb{R}^{n_x \times n_x}$, $e_G = \hat{G} - G \in \mathbb{R}^{n_x \times n_z}$, and $e_H = \hat{H} - H \in \mathbb{R}^{n_z \times n_x}$. As f , g , and h are assumed to be continuously differentiable, the Jacobians, F , G , and H , are continuous and since the steady state of the approximate system converges to that of the original system as $a_i \rightarrow \infty$ and $M_i/a_i \rightarrow \infty$, the errors e_F , e_G , and e_H converge to zero. The norm of the integral in the third term is

$$\begin{aligned}
(4.44) \quad & \left\| \int_0^\infty e^{-\lambda s} \text{diag}(\hat{\alpha}(s) - \alpha(s)) \, ds \right\|_\infty = \max_{i=1, \dots, n_z} \left| \int_0^\infty e^{-\lambda s} (\hat{\alpha}_i(s) - \alpha_i(s)) \, ds \right| \\
&\leq \max_{i=1, \dots, n_z} \int_0^\infty |e^{-\lambda s}| |\hat{\alpha}_i(s) - \alpha_i(s)| \, ds.
\end{aligned}$$

As we have shown above, for any $\lambda \in \mathbb{C}$ for which $\text{Re } \lambda > \lambda_{\min}$, we can choose s_0 , \bar{a} , and \bar{M} (for which $\bar{M}/\bar{a} \rightarrow \infty$ as $\bar{a} \rightarrow \infty$) such that this expression is below any $\epsilon \in \mathbb{R}_{>0}$ whenever $a_i > \bar{a}$ and $M_i > \bar{M}$ for $i = 1, \dots, n_z$, which concludes the proof. \blacksquare

Lemma 4.10. *Let the elements of $\alpha : \mathbb{R}_{\geq 0} \rightarrow \mathbb{R}^{n_z}$ be exponentially bounded and regular, i.e., let there exist $L, \rho \in \mathbb{R}_{>0}$ such that $|\alpha_i(t)| \leq L e^{-\rho t}$ for all $t \in \mathbb{R}_{\geq 0}$ and $i = 1, \dots, n_z$, and let the i 'th element of $\hat{\alpha} : \mathbb{R}_{\geq 0} \rightarrow \mathbb{R}^{n_z}$ be the Erlang mixture approximation of α_i of order $M_i \in \mathbb{N}_{\geq 0}$ with rate parameter $a_i \in \mathbb{R}_{>0}$. Then, the characteristic function $\hat{P} : \mathbb{C} \rightarrow \mathbb{C}$ defined by (4.26) is holomorphic for $\lambda \in \mathbb{C}$ for which $\text{Re } \lambda > -\rho$.*

Proof. We prove that the complex derivatives of the diagonal entries of the auxiliary matrix $Q : \mathbb{C} \rightarrow \mathbb{C}^{n_z \times n_z}$ defined in (4.26) exist for an arbitrary point and direction $\lambda_0, \Delta\lambda \in \mathbb{C}$, i.e., for $\lambda = \lambda_0 + w\Delta\lambda$ where $w \in \mathbb{R}_{\geq 0}$. We derive the derivative from the expression in Corollary 4.8:

$$(4.45) \quad \frac{\partial Q_{ii}}{\partial w}(\lambda) = - \int_0^\infty \frac{\partial \lambda}{\partial w} s e^{-\lambda s} \hat{\alpha}_i(s) \, ds = -\Delta\lambda \int_0^\infty s e^{-\lambda s} \hat{\alpha}_i(s) \, ds.$$

The derivative exists if the integral is finite. According to Corollary 4.3, $\hat{\alpha}_i$ is exponentially bounded if α_i is. Specifically, $\hat{\alpha}_i(t) \leq L e^{-\bar{\rho} t}$ for all t where $0 \leq \bar{\rho} < \rho$. Consequently,

$$(4.46) \quad \left| \int_0^\infty s e^{-\lambda s} \hat{\alpha}_i(s) \, ds \right| \leq \int_0^\infty s e^{-\text{Re } \lambda s} L e^{-\bar{\rho} s} \, ds = L \int_0^\infty s e^{-(\text{Re } \lambda + \bar{\rho})s} \, ds = \frac{L}{(\text{Re } \lambda + \bar{\rho})^2}$$

for $\operatorname{Re} \lambda > -\bar{\rho}$. Furthermore, for any λ for which $\operatorname{Re} \lambda > -\rho$, we can choose \bar{a} and \bar{M} (for which $\bar{M}/\bar{a} \rightarrow \infty$ as $\bar{a} \rightarrow \infty$) large enough that $\operatorname{Re} \lambda > -\bar{\rho} > -\rho$ whenever $a_i > \bar{a}$ and $M_i > \bar{M}$ for $i = 1, \dots, n_z$. Consequently, the derivative exists when $\operatorname{Re} \lambda > -\rho$. Finally, as the determinant of a holomorphic function is also holomorphic and the remaining terms in the argument of the determinant in the expression for \hat{P} in (4.26) are constant and linear in λ , \hat{P} is holomorphic when $\operatorname{Re} \lambda > \rho$. ■

Proof of Theorem 4.4(b). According to Lemma 4.10 and 4.9, respectively, \hat{P} is holomorphic and converges uniformly to P for $\lambda \in \mathbb{C}$ with real part larger than or equal to λ_{\min} . Consequently, the convergence of the roots of \hat{P} follows from Hurwitz' convergence theorem [19, Thm. 5.6.4] since the roots are isolated by assumption. ■

4.4. Error dynamics. In this section, we analyze the difference between the solution to the IVP (4.7)–(4.8) involving approximate ODEs and that of the original IVP (3.1)–(3.2) involving DDEs, and we show that for a given time $t \in [t_0, t_f]$, it converges to zero as the Erlang mixture approximation becomes more accurate.

First, we introduce the state error, $e_x : \mathbb{R} \rightarrow \mathbb{R}^{n_x}$, the error of the memory state and the delayed variable, $e_z, e_r : \mathbb{R} \rightarrow \mathbb{R}^{n_z}$, and the kernel error, $e_\alpha : \mathbb{R}_{\geq 0} \rightarrow \mathbb{R}^{n_z}$, given by

$$(4.47) \quad e_x(t) = \hat{x}(t) - x(t), \quad e_z(t) = \hat{z}(t) - z(t), \quad e_r(t) = \hat{r}(t) - r(t), \quad e_\alpha(t) = \hat{\alpha}(t) - \alpha(t),$$

where \hat{x} and \hat{z} are the solution to the IVP (4.7)–(4.8) involving ODEs and x and z are the solution to the original IVP (3.1)–(3.2) involving DDEs. The state error satisfies the IVP

$$(4.48a) \quad e_x(t) = 0, \quad t \in (-\infty, t_0],$$

$$(4.48b) \quad \dot{e}_x(t) = f(\hat{x}(t), \hat{z}(t)) - f(x(t), z(t)), \quad t \in [t_0, t_f].$$

Proof of Theorem 4.4(c). The steady states of the original and approximate system are not identical (see Lemma 4.6). Consequently, the steady state of the error, $\bar{e}_x \in \mathbb{R}^{n_x}$, will not be zero. The linearized system corresponding to the DDE (4.48b) describing the state error is

$$(4.49) \quad \dot{E}_x(t) = \hat{F}\hat{X}(t) + \hat{G} \int_{-\infty}^t \hat{\alpha}(t-s) \odot \hat{H}\hat{X}(s) ds - \left(FX(t) + G \int_{-\infty}^t \alpha(t-s) \odot HX(s) ds \right),$$

where $E_x : \mathbb{R} \rightarrow \mathbb{R}^{n_x}$ is the deviation from the steady state error, i.e., $E_x(t) = e_x(t) - \bar{e}_x$, and $\hat{X}, X : \mathbb{R} \rightarrow \mathbb{R}^{n_x}$ are the deviations of the state variables from their respective steady states. Next, we rewrite the system by adding and subtracting terms such that \hat{X} does not appear on the right-hand side:

$$(4.50) \quad \begin{aligned} \dot{E}_x(t) = & \hat{F}E_x(t) + e_F X(t) + G \int_{-\infty}^t \hat{\alpha}(t-s) \odot \hat{H}E_x(s) ds + \hat{G} \int_{-\infty}^t \hat{\alpha}(t-s) \odot e_H X(s) ds \\ & + \hat{G} \int_{-\infty}^t e_\alpha(t-s) \odot HX(s) ds + e_G \int_{-\infty}^t \alpha(t-s) \odot HX(s) ds. \end{aligned}$$

As the system depends on the deviation, X , of the state variables from the steady state, \bar{x} , the stability cannot be investigated independently. Therefore, we augment it with the linearized system (3.8) to obtain

$$(4.51) \quad \begin{bmatrix} \dot{X}(t) \\ \dot{E}_x(t) \end{bmatrix} = \begin{bmatrix} F \\ e_F & \hat{F} \end{bmatrix} \begin{bmatrix} X(t) \\ E_x(t) \end{bmatrix} + \begin{bmatrix} G \\ e_G & \hat{G} \end{bmatrix} \int_{-\infty}^t \begin{bmatrix} \text{diag } \alpha(t-s) & \\ \text{diag } e_\alpha(t-s) & \text{diag } \hat{\alpha}(t-s) \end{bmatrix} \begin{bmatrix} H \\ e_H & \hat{H} \end{bmatrix} \begin{bmatrix} X(s) \\ E_x(s) \end{bmatrix} ds.$$

The corresponding characteristic function is

$$(4.52) \quad \det \left(\begin{bmatrix} F & \\ e_F & \hat{F} \end{bmatrix} - \begin{bmatrix} \lambda I & \\ & \lambda I \end{bmatrix} + \begin{bmatrix} G & \\ e_G & \hat{G} \end{bmatrix} \int_0^\infty e^{-\lambda s} \begin{bmatrix} \text{diag } \alpha(s) & \\ \text{diag } e_\alpha(s) & \text{diag } \hat{\alpha}(s) \end{bmatrix} ds \begin{bmatrix} H \\ e_H & \hat{H} \end{bmatrix} \right) \\ = \det(F - \lambda I + G \int_0^\infty e^{-\lambda s} \text{diag } \alpha(s) ds H) \det(\hat{F} - \lambda I + \hat{G} \int_0^\infty e^{-\lambda s} \text{diag } \hat{\alpha}(s) ds \hat{H}) \\ = P(\lambda) \hat{P}(\lambda),$$

where P and \hat{P} are the characteristic functions corresponding to the original system of DDEs (3.1b)–(3.2) and the approximate system of ODEs (4.7), respectively. Consequently, the roots of P and \hat{P} are also roots of the above characteristic function, and if their real parts are negative, the augmented system is asymptotically stable and the error dynamics are locally asymptotically stable. ■

4.5. Uniform convergence. In this section, we prove Theorem 4.4(d) on the uniform convergence of the solution to the IVP (4.7)–(4.8) involving ODEs to the solution of the original IVP (3.1)–(3.2) involving DDEs.

Proof of Theorem 4.4(d). First, we prove that the solution, \hat{x} , to the IVP (4.7)–(4.8) with ODEs converges uniformly to that of the IVP (3.1)–(3.2) with DDEs. According to Proposition 4.2(d), we can choose \bar{a} and \bar{M} large enough that

$$(4.53) \quad \int_0^\infty \|e_\alpha(t)\|_\infty dt < \epsilon$$

when $a_i > \bar{a}$ and $M_i > \bar{M}$ for $i = 1, \dots, n_z$ provided that $\bar{M}/\bar{a} \rightarrow \infty$ as $\bar{a} \rightarrow \infty$. Furthermore, since 1) the delayed variable, r , is assumed to be bounded and 2) the functions f and h are assumed to be differentiable (and thus also Lipschitz continuous), the result follows from a proof similar to that of Theorem 1 in the paper by Guglielmi and Hairer [18]. For completeness, we present the details of the proof in Section SM3 of the supplementary material. Specifically,

$$(4.54) \quad \|e_x(t)\|_\infty \leq \epsilon w(t) \leq \epsilon w(t_f),$$

where the auxiliary function $w : \mathbb{R} \rightarrow \mathbb{R}_{\geq 0}$ is the solution to the DDE

$$(4.55a) \quad w(t_0) = 0,$$

$$(4.55b) \quad \dot{w}(t) = L_z K_r + L_x w(t) + L_z L_r \int_{t_0}^t \|\hat{\alpha}(t-s)\|_\infty w(s) ds, \quad t \in [t_0, t_f],$$

and $L_x \in \mathbb{R}_{>0}$ and $L_z \in \mathbb{R}_{>0}$ are the Lipschitz constants of the first and second arguments of f , and $L_r \in \mathbb{R}_{>0}$ is the Lipschitz constant of h . Furthermore, K_r is the supremum of the absolute value of r in the time interval $(-\infty, t_f]$ (see also the assumptions in Section 3). The second inequality in (4.54) follows from the non-negativity of the right-hand side of the DDE (4.55b) and ensures that the convergence is uniform on the time interval $[t_0, t_f]$. In conclusion, the state error, e_x , can be made arbitrarily small by making the kernel error sufficiently small.

Next, we prove that \hat{z} and \hat{r} converge uniformly. As h is differentiable, $|e_{r,i}(t)| \leq L_r |e_{x,i}(t)| \leq L_r \epsilon w(t_f)$, and therefore, the convergence of \hat{r} is uniform. We bound the integral of the absolute value of the i 'th Erlang mixture approximation by

$$(4.56) \quad \begin{aligned} \int_0^\infty |\hat{\alpha}_i(t)| dt &\leq \sum_{m=0}^M |c_m| \int_0^\infty \ell_m(t) dt = \sum_{m=0}^M |c_m| \leq \sum_{m=0}^M \int_{s_m}^{s_{m+1}} |\alpha(t)| dt \\ &= \int_0^{s_{M+1}} |\alpha(t)| dt \leq \rho(\infty), \end{aligned}$$

which is finite by assumption. Using these two bounds, we derive a bound on the absolute memory state error:

$$(4.57) \quad \begin{aligned} |e_{z,i}(t)| &= \left| \int_{-\infty}^t \hat{\alpha}_i(t-s) \hat{r}_i(s) ds - \int_{-\infty}^t \alpha_i(t-s) r_i(s) ds \right| \\ &= \left| \int_{-\infty}^t \hat{\alpha}_i(t-s) e_{r,i}(s) ds + \int_{-\infty}^t e_{\alpha,i}(t-s) r_i(s) ds \right| \\ &\leq \int_{-\infty}^t |\hat{\alpha}_i(t-s)| |e_{r,i}(s)| ds + \int_{-\infty}^t |e_{\alpha,i}(t-s)| |r_i(s)| ds \\ &\leq \int_{-\infty}^t |\hat{\alpha}_i(t-s)| ds \sup_{s \in (-\infty, t]} |e_{r,i}(s)| + \int_{-\infty}^t |e_{\alpha,i}(t-s)| ds \sup_{s \in (-\infty, t]} |r_i(s)| \\ &\leq (\rho(\infty) L_r w(t_f) + K_r) \epsilon. \end{aligned}$$

From the first to the second equality, we add and subtract the integral of $\hat{\alpha}_i(t-s)r_i(s)$ (i.e., a mixed term). In conclusion, we can bound the pointwise error, and the bound is independent of t for $t \in (-\infty, t_f]$, i.e., the convergence is uniform over that interval. \blacksquare

5. Algorithm. In this section, we describe an algorithm for determining the coefficients and the rate parameter in an M 'th order Erlang mixture approximation of a regular kernel, $\alpha : \mathbb{R}_{\geq 0} \rightarrow \mathbb{R}$, for given $M \in \mathbb{N}_{\geq 0}$. For simplicity, we only consider scalar kernels in this section. The algorithm consists of two steps: First, we identify a domain in which we approximate the kernel and then, we use a least-squares approach to determine the coefficients. Furthermore, we describe a reference approach based on the theoretical expressions in (4.3) for the coefficients. Finally, we describe the implementation of the algorithm and the simulation of the original DDEs (3.1b)–(3.2) and the approximate system of ODEs (4.7).

5.1. Domain. In order to determine the approximation domain, we choose $t_h \in \mathbb{R}_{\geq 0}$ as the solution to the equation $\rho(\infty) - \rho(t) = \epsilon$ for a given threshold, $\epsilon \in \mathbb{R}_{>0}$, and approximate α in the interval $[0, t_h]$. We use bisection to determine t_h approximately. We assume that an

initial interval, $[t_0^\ell, t_0^u]$, is available and that it contains the root, i.e., that $\rho(\infty) - \rho(t_0^\ell) > \epsilon$ and $\rho(\infty) - \rho(t_0^u) < \epsilon$. If that is not the case, the interval can be shifted or scaled such that it does. Next, the k 'th iteration has converged and an approximate solution has been found if $|\rho(\infty) - \rho(t_k^m) - \epsilon|$ is below a specified threshold, where $t_k^m = \frac{1}{2}(t_k^\ell + t_k^u)$ is the midpoint. Otherwise, the next iteration considers the lower half of the interval, $[t_{k+1}^\ell, t_{k+1}^u] = [t_k^\ell, t_k^m]$, if $\rho(\infty) - \rho(t_k^m) < \epsilon$. Conversely, if $\rho(\infty) - \rho(t_k^m) > \epsilon$, the next iteration considers the upper half of the interval, $[t_{k+1}^\ell, t_{k+1}^u] = [t_k^m, t_k^u]$.

Remark 5.1. If the function ρ in (3.3) cannot be derived analytically for a given kernel, α , it can be approximated using numerical quadrature (e.g., with MATLAB's function `integral`).

Remark 5.2. The equation $\rho(\infty) - \rho(t) = \epsilon$ can also be solved using a gradient-based approach, e.g., Newton's method. However, $\rho(\infty) - \rho(t)$ rounds to zero in finite-precision arithmetic when t is too large, e.g., in a computer implementation. Consequently, Newton iterations may stall if an iterate happens to become too large.

5.2. Identify kernel parameters. For a given order, $M \in \mathbb{N}_{\geq 0}$, and $t_h \in \mathbb{R}_{\geq 0}$, we choose the rate parameter $a \in \mathbb{R}_{> 0}$ as

$$(5.1) \quad a = \frac{M + 1}{t_h}.$$

Next, the objective is to determine the values of the coefficients, $c_m \in \mathbb{R}$ for $m = 0, \dots, M$, that minimize the integral of the squared error over the interval $[0, t_h]$,

$$(5.2) \quad \int_0^{t_h} (\alpha(t) - \hat{\alpha}(t))^2 dt,$$

while satisfying the constraint that the coefficients must sum to the integral of α over the same interval. We approximate this integral by a left rectangle rule (such that the objective function includes $\alpha(0)$) with N rectangles, and we determine the coefficients by solving the regularized and constrained quadratic program (QP)

$$(5.3a) \quad \min_{\{c_m\}_{m=0}^M} \phi = \frac{1}{2} \sum_{k=0}^{N-1} (\alpha(t_k) - \hat{\alpha}(t_k))^2 \Delta t + \frac{w}{2} \sum_{m=0}^M c_m^2,$$

$$(5.3b) \quad \text{subject to} \quad \sum_{m=0}^M c_m = \beta(t_h),$$

where the quadrature points are $t_k = k\Delta t$ for $k = 0, \dots, N - 1$, $\Delta t \in \mathbb{R}_{> 0}$ is the width of the rectangles, and $w \in \mathbb{R}_{> 0}$ is a regularization weight. Furthermore, the objective function involves the regular kernel, $\alpha : \mathbb{R}_{\geq 0} \rightarrow \mathbb{R}$, and the M 'th order Erlang mixture kernel, $\hat{\alpha} : \mathbb{R}_{\geq 0} \rightarrow \mathbb{R}$, with coefficients $\{c_m\}_{m=0}^M$ and rate parameter a , evaluated at the quadrature points.

Proposition 5.3. *The unique solution $c \in \mathbb{R}^{M+1}$ to the regularized and constrained least-squares problem (5.3) is a column vector given by*

$$(5.4) \quad c = (L^T L + wI)^{-1}(e\lambda + L^T g),$$

where $\lambda \in \mathbb{R}$ is a Lagrange multiplier, $e \in \mathbb{R}^{M+1}$ is a column vector of ones, and $L \in \mathbb{R}_{\geq 0}^{N \times M+1}$ and $g \in \mathbb{R}^N$ are a matrix and vector whose elements are equal to the basis functions and the kernel α evaluated in the quadrature points, respectively:

$$(5.5) \quad \lambda = \frac{\beta(t_h) - e^T(L^T L + wI)^{-1} L^T g}{e^T(L^T L + wI)^{-1} e}, \quad L_{km} = \ell_m(t_k), \quad g_k = \alpha(t_k),$$

for $m = 0, \dots, M$ and $k = 0, \dots, N - 1$.

Proof. The QP (5.3) is in the form

$$(5.6a) \quad \min_c \quad \phi = \frac{1}{2} c^T (L^T L + wI) c + g^T L c,$$

$$(5.6b) \quad \text{subject to} \quad e^T c = \beta(t_h),$$

where $I \in \mathbb{R}^{M+1 \times M+1}$ is an identity matrix. This is an equality-constrained quadratic program and the first-order necessary conditions for a solution is that there must exist a Lagrange multiplier, λ , such that the following linear system of equations is satisfied [38, Sec. 16.1]:

$$(5.7) \quad \begin{bmatrix} L^T L + wI & -e \\ -e^T & \end{bmatrix} \begin{bmatrix} c \\ \lambda \end{bmatrix} = \begin{bmatrix} L^T g \\ -\beta(t_h) \end{bmatrix}.$$

The expression for c in (5.4) is the solution to the first row block. Next, we substitute it into the second row block:

$$(5.8) \quad -e^T c = -e^T (L^T L + wI)^{-1} (e\lambda + L^T g) = -\beta(t_h).$$

The expression for λ in (5.5) is obtained by isolating λ in the rightmost equation. Finally, the solution is locally unique because the Hessian $L^T L + wI$ is positive definite when $w > 0$, i.e., $x^T (L^T L + wI) x = \|Lx\|_2^2 + w\|x\|_2^2 > 0$ for all $x \neq 0$ [38, Thm. 12.6]. ■

5.3. Theoretical Erlang mixture approximation. We will compare the accuracy obtained with the least-squares approach described in Section 5.2 to that of a reference approach based on the theoretical values of the coefficients from Proposition 4.2. First, we determine the size of the approximation interval, t_h , such that $\rho(\infty) - \rho(t_h) \approx \epsilon$, e.g., using bisection as described in Section 5.1. Next, for a given order, M , we determine the rate parameter by (5.1), and we use the theoretical expression in (4.3) to compute the coefficients, c_m , for $m = 0, \dots, M$.

5.4. Implementation. We exploit that the recursion $\ell_m(t) = (at/m)\ell_{m-1}(t)$ for $m = 1, \dots, M$ where $\ell_0(t) = ae^{-at}$ is less prone to rounding errors than a straightforward evaluation of the expression (4.1) in the definition. We simulate the approximate system of ODEs (4.7) using either MATLAB's `ode45` or `ode15s`, and depending on the order of the Erlang mixture kernel, we implement the matrices A , B , and C as either dense or sparse. Furthermore, we provide the analytical Jacobian of the right-hand side function of the approximate system of ODEs (4.7) to the simulator. We implement the numerical method for non-stiff DDEs described in Appendix G.1 in both MATLAB and C (with a MEX interface). The numerical method from Appendix G.2 is implemented in MATLAB, we use `fsolve` to solve the residual equations, and we provide the analytical Jacobian. In all three implementations, the right-hand side function, f , the delay function, h , and the kernel, α , are evaluated in MATLAB. Finally, in Section 7, we carry out parallel simulations and kernel approximations using a high-performance computing cluster [14].

6. Numerical test of the accuracy. In this section, we construct a DDE in the form (3.1b)–(3.2) with a known solution and use it to investigate the accuracy of the Erlang mixture approximation and the numerical solution of the approximate system of ODEs (4.7). Furthermore, we assess the convergence rate of the two numerical methods for solving IVPs in the form (3.1)–(3.2) described in Appendix G. Finally, we compare the accuracy of the Erlang mixture approximation with that of one of the exponential mixture approximations described in [18] for a system of DDEs involving a gamma kernel, which describes chemotherapy-induced myelosuppression [32].

6.1. Modified logistic equation. We consider a modified logistic differential equation with a forcing term in the form

$$(6.1) \quad \dot{x}(t) = \sigma x(t) \left(1 - \frac{z(t)}{\kappa}\right) + Q(t), \quad z(t) = \int_{-\infty}^t \alpha(t-s)x(s) ds.$$

Here, $x : \mathbb{R} \rightarrow \mathbb{R}_{\geq 0}$ is a population density, $z : \mathbb{R} \rightarrow \mathbb{R}_{\geq 0}$ is the memory state, $\sigma \in \mathbb{R}_{> 0}$ is the logistic growth rate, $\kappa \in \mathbb{R}_{> 0}$ is a carrying capacity, and $Q : \mathbb{R} \rightarrow \mathbb{R}$ is the forcing term. We choose the solution, $x^* : \mathbb{R} \rightarrow \mathbb{R}_{\geq 0}$, and the kernel, $\alpha : \mathbb{R}_{\geq 0} \rightarrow \mathbb{R}_{\geq 0}$, as

$$(6.2) \quad x^*(t) = 1 + e^{-\left(\frac{t}{\gamma}\right)^2}, \quad \alpha(t) = \frac{2}{\sqrt{\pi}} e^{-t^2}, \quad \beta(t) = \operatorname{erf}(t),$$

where $\gamma \in \mathbb{R}_{> 0}$ is a dilation parameter, $\beta : \mathbb{R}_{\geq 0} \rightarrow [0, 1]$ is derived from (3.3), and $\operatorname{erf} : \mathbb{R} \rightarrow [0, 1]$ is the error function. Consequently, the true memory state, $z^* : \mathbb{R} \rightarrow \mathbb{R}_{\geq 0}$, is

$$(6.3) \quad z^*(t) = 1 + \frac{\gamma}{\sqrt{\gamma^2 + 1}} e^{-\frac{t^2}{\gamma^2 + 1}} \left(1 + \operatorname{erf}\left(\frac{t}{\gamma\sqrt{\gamma^2 + 1}}\right)\right),$$

and the forcing term is chosen such that x^* in (6.2) is the solution:

$$(6.4) \quad Q(t) = \dot{x}^*(t) - \sigma x^*(t) \left(1 - \frac{z^*(t)}{\kappa}\right).$$

This is referred to as the *method of manufactured solutions* [45].

Remark 6.1. We choose x^* such that it is bounded away from zero because the system becomes unstable if the numerical approximation of the solution becomes negative. This can happen when the true solution is close to zero, in which case the numerical approximation may diverge.

Figure 2 shows the approximation errors for the state and the kernel:

$$(6.5) \quad E_x = \left(\sum_{n=0}^{N_x-1} (\hat{x}(t_{n+1}) - x^*(t_{n+1}))^2 \Delta t_x \right)^{\frac{1}{2}}, \quad E_\alpha = \left(\sum_{k=0}^{N_\alpha-1} (\hat{\alpha}(t_k) - \alpha(t_k))^2 \Delta t_\alpha \right)^{\frac{1}{2}}.$$

Here, \hat{x} and $\hat{\alpha}$ denote the approximations, and $\Delta t_x = (t_f - t_0)/N_x$ and $\Delta t_\alpha = t_h/N_\alpha$. Note that the kernel error, E_α , is analogous to the square root of the first term in the objective

function in (5.3a) but may contain a different number of terms. We have used the model parameter values $\sigma = 4 \text{ mo}^{-1}$ and $\kappa = 1$ and the dilation parameter $\gamma = 10 \text{ mo}$, and the initial and final times are $t_0 = 0 \text{ mo}$ and $t_f = 24 \text{ mo}$. When we determine the Erlang mixture approximation of a given order, M , we use $N = 10^3$ points in the objective function in (5.3a). Furthermore, we use a threshold of $\epsilon = 10^{-14}$ and a convergence tolerance of 10^{-15} to determine the approximation interval length, t_h (see Table 1). We also use the identified value of t_h in the reference approach described in Section 5.3. We use MATLAB's `ode45` with absolute and relative tolerances of 10^{-12} to simulate the approximate system of ODEs (4.7), and we use $N_x = 24 \cdot 10^3$ quadrature points to evaluate the state error in (6.5), which corresponds to a time step size of $\Delta t_x = 10^{-3} \text{ mo}$. Furthermore, we use $N_\alpha = 10^6$ quadrature points to evaluate the kernel error. For the results obtained with the numerical methods described in Appendix G, we use a memory horizon of $\Delta t_h = t_f - t_0 = 24 \text{ mo}$ and the above time step size, and for the method for stiff DDEs, we use a function tolerance of 10^{-12} and an optimality tolerance of 10^{-8} when we solve the involved residual equations with MATLAB's `fsolve`.

The results demonstrate that for this example, the Erlang mixture approximation obtained with the proposed least-squares approach is several orders of magnitude more accurate than the reference approach based on the theoretical expressions for the coefficients. In both cases, there is a high correlation between the error of the kernel and the error of the approximate state trajectory. For the least-squares approach, the convergence rates are faster than polynomial, and for the reference approach, the convergence rates are linear for sufficiently large values of M (see also Figure SM1). The kernel error is higher for M equal to 128 than for 64 because the objective function in the QP (5.3) uses a coarser resolution in the rectangle rule than the error in (6.5). Finally, the state error decreases linearly with the time step size for the two numerical methods described in Appendix G because the involved integral and differential equation have been discretized with first-order methods.

6.2. Myelosuppression. In this section, we compare the accuracy of the Erlang mixture approximation proposed in this work with an exponential mixture approximation (see Section SM4) used by Guglielmi and Hairer [18] for a system of DDEs describing myelosuppression. The system describes the evolution of precursor cells, $y : \mathbb{R} \rightarrow \mathbb{R}_{\geq 0}$, which ultimately form granulocytes, $w : \mathbb{R} \rightarrow \mathbb{R}_{\geq 0}$:

$$(6.6a) \quad \dot{y}(t) = \left(\kappa \left(\frac{w_0}{w(t)} \right)^\gamma - k_s C(t) - \kappa \right) y(t),$$

$$(6.6b) \quad \dot{w}(t) = -\kappa w(t) + \kappa \int_{-\infty}^t \alpha(t-s) y(s) ds,$$

$$(6.6c) \quad \dot{C}(t) = -\frac{V_{\max} C(t)}{K_m + C(t)}.$$

The purpose of the model is to study the effect of a bolus injection of a drug (fluoracil) and $C : \mathbb{R} \rightarrow \mathbb{R}_{\geq 0}$ is the concentration of the drug in the plasma, which is described by the Michaelis-Menten model in (6.6c). The constants are $\kappa = (1 - \lambda)/55.6 \text{ h}^{-1}$, $\lambda = -0.46$, $w_0 = 14.4 \cdot 10^9 \text{ cells/L}$, $\gamma = 0.507$, $k_s = 0.0213 \text{ L/(mg h)}$, $V_{\max} = 100 \text{ mg/(L h)}$, and

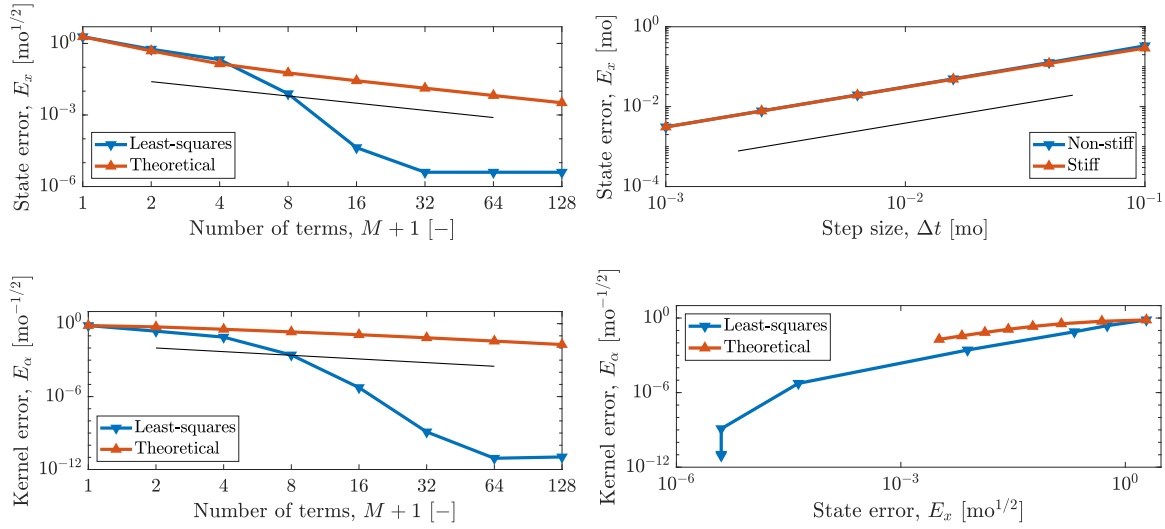


Figure 2. Convergence analysis for the modified logistic equation. The state (top left) and kernel (bottom left) errors for Erlang mixture approximations of different orders, M , obtained with the proposed least-squares approach and the reference approach based on the theoretical expressions for the coefficients. The bottom right plot shows the state and kernel errors against each other, and the top right plot shows the state error obtained with the numerical approaches for non-stiff and stiff DDEs for different time step sizes, Δt . The black solid lines in the left column are proportional to $1/(M+1)$, and the one in the top right is proportional to Δt .

$K_m = 22 \text{ mg/L}$, and the gamma kernel is given by

$$(6.7) \quad \alpha(t) = \frac{\kappa^{1-\lambda}}{\Gamma(1-\lambda)} t^{-\lambda} e^{-\kappa t},$$

where $\Gamma : \mathbb{C} \rightarrow \mathbb{C}$ is the gamma function. The initial and final times are $t_0 = 0 \text{ h}$ and $t_f = 700 \text{ h}$, and the initial states are $y(t) = w_0$ for $t \in (-\infty, t_0]$, $w(t_0) = w_0$, and $C(t_0) = A_0/V$ where $A_0 = 127 \text{ mg/kg}$ and $V = 1.03 \text{ L/kg}$. We use a threshold of $\epsilon = 10^{-3}$ in the computation of t_h (see Table 1), and we use $N = 10^4$ points in the objective function. The initial guess of the rate parameter, a , is κ . As the system is stiff, we use `ode15s` to simulate the approximate system of ODEs (4.7), and we compare to the error of the exponential mixture approximation described in [18], which depends on the tolerance $\epsilon_r \in \mathbb{R}_{>0}$ that also indirectly determines the number of terms in the approximation. Lower tolerances lead to more terms, and we consider $\epsilon_r \in \{10^{-1}, 10^{-3}, 10^{-5}, 10^{-7}, 10^{-9}, 10^{-11}\}$. Furthermore, we compare the state obtained with the Erlang mixture approach to that obtained with $\epsilon_r = 10^{-11}$ using $N_x = 700 \cdot 10^3$ points in time, corresponding to a time step size of $\Delta t_x = 10^{-3} \text{ h}$. The remaining parameters are the same as in Section 6.1.

The results are shown in Figure 3, and as for the example in Section 6.1, the least-squares approach described in Section 5 is significantly more accurate than the reference approach based on the theoretical expressions for the coefficients. However, the error is generally higher than for the modified logistic equation (see Figure 2), the convergence rates are no longer faster than polynomial for the least-squares approach, and they are no longer linear for the reference approach based on the theoretical expressions for the coefficients. The

Table 1

The Erlang mixture approximation order, M , the approximation horizon, t_h , identified with the bisection method from Section 5.1, and the value of the rate parameter, a , obtained with (5.1) for the problems considered in Section 6 (the first two) and Section 7. For the first two problems, t_h is fixed, but M varies. Therefore, a varies as well, and this is marked with a v . The third and fourth problems are the bifurcation analyses with respect to the logistic growth rate, σ , and the kernel parameter, μ_2 , respectively, and in the latter case, the shown values correspond to the six values of μ_2 considered in Figure 4 and 5. The fifth problem involves the six kernels shown in Figure 7.

Problem	M	t_h	a
Modified logistic equation (forced)	v	4.32 mo	v
Myelosuppression	v	489.08 h	v
Modified logistic equation (σ)	100	1.36 mo	74.41 mo^{-1}
Modified logistic equation (μ_2)	350	0.92 mo	380.75 mo^{-1}
		1.22 mo	287.08 mo^{-1}
		1.45 mo	242.85 mo^{-1}
		1.62 mo	217.31 mo^{-1}
		1.91 mo	184.13 mo^{-1}
		2.32 mo	151.27 mo^{-1}
Nuclear fission	500	12.13 s	41.32 s^{-1}
		12.10 s	41.43 s^{-1}
		11.97 s	41.86 s^{-1}
		11.69 s	42.87 s^{-1}
		10.53 s	47.57 s^{-1}
		8.28 s	60.50 s^{-1}

figure also shows that Guglielmi and Hairer's approach does have converge rates that are faster than polynomial (note the difference in the vertical axes). The error of the Erlang mixture approximation is primarily high for t close to zero. The reason for this may be that the derivative of the true kernel has a singularity at zero whereas for finite values of M and a , the derivative of the Erlang mixture approximation does not. This may also describe why the convergence rates of the Erlang mixture approximation are reduced. However, we emphasize that the Erlang mixture approximation can be used for a broader class of kernels (bounded and continuous) than the exponential mixture approximations. Furthermore, the state error is generally high because of the order of magnitude of the state variables (10–30 for y and w) and the length of the simulation interval. A constant error of 1 would correspond to a state error of $E_x = \sqrt{700} \approx 26.5$. Even for $M + 1 = 4$, the state error is below this value.

7. Numerical examples. In this section, we present two numerical examples that demonstrate how Erlang mixture approximations can be used to approximately analyze and simulate DDEs with distributed time delays. In the first example, we use the approximate system of ODEs (4.7) to perform a numerical bifurcation analysis of the modified logistic differential equation that was also considered in Section 6, and in the second example, we present a Monte Carlo simulation of a molten salt nuclear fission process, which is nonlinear, multivariate, and stiff. We use high orders, M , and strict tolerances in the numerical methods to mitigate any adverse effects on the results. However, in many practical contexts, lower orders and less restrictive tolerances can be used with limited effect on the accuracy (see also Section 6).

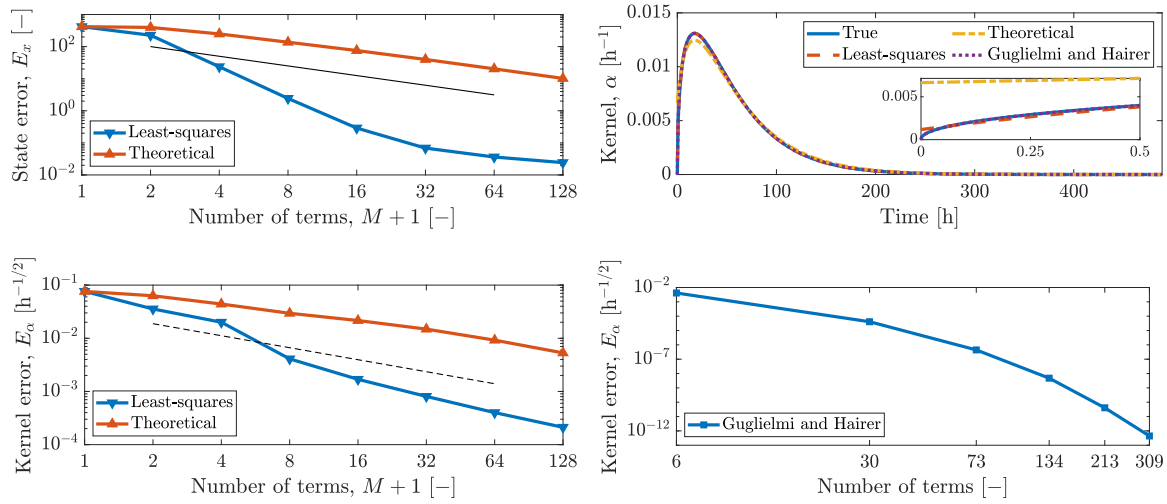


Figure 3. Convergence analysis for the myelosuppression model. The maximum state error (top left) and the kernel error (bottom left) for Erlang mixture approximations of different orders, M , obtained with the least-squares approach and the reference approach based on theoretical values of the coefficients. The kernel error is shown for Guglielmi and Hairer's approach in the bottom right, and the true and approximate kernels are shown in the top right for $M = 128$ and $\epsilon_r = 10^{-11}$ (corresponding to 309 terms). The black solid line in the top left is proportional to $1/(M+1)$ whereas the black dashed line in the bottom left is proportional to $1/(M+1)^{3/4}$.

7.1. Modified logistic equation. We consider the modified logistic differential equation (6.1) where the forcing term is $Q(t) = 0$ and the kernel is

$$(7.1) \quad \alpha(t) = \gamma_1 F(t; \mu_1, \sigma_1) + \gamma_2 F(t; \mu_2, \sigma_2).$$

Here, $\gamma_1, \gamma_2 \in [0, 1]$ are weights, $\mu_1, \mu_2 \in \mathbb{R}$ are location parameters, $\sigma_1, \sigma_2 \in \mathbb{R}_{>0}$ are scale parameters, and $F : \mathbb{R}_{\geq 0} \times \mathbb{R} \times \mathbb{R}_{>0} \rightarrow \mathbb{R}_{\geq 0}$ is given by the probability density function of a folded normal distribution (i.e., it is a folded normal kernel):

$$(7.2) \quad F(t; \mu_i, \sigma_i) = \frac{\exp\left(-\frac{1}{2}\left(\frac{t-\mu_i}{\sigma_i}\right)^2\right) + \exp\left(-\frac{1}{2}\left(\frac{t+\mu_i}{\sigma_i}\right)^2\right)}{\sqrt{2\pi}\sigma_i}, \quad i = 1, 2.$$

Furthermore, we derive β in Definition 3.1 analytically.

We use the parameter values in Table 2, and the initial state is $x(t) = 0.9$ for $t \leq t_0$. We use the same parameters as in Section 6.1 to identify Erlang mixture kernels of order $M = 100$ in the bifurcation analysis with respect to the logistic growth rate, σ , and $M = 350$ in the analysis with respect to the kernel parameter μ_2 . Table 1 shows the resulting values of t_h and a . In Figure 4, the first row shows the eigenvalues of the Jacobian of the right-hand side function in the approximate system of ODEs (4.7). For completeness, we consider a large range of values for σ , but for numerical reasons, we have not been able to investigate larger values of μ_2 . The second row shows the largest real part of the eigenvalues and when the parameters become sufficiently large, the steady state $\bar{x} = \kappa$ becomes unstable. The two bottom rows show simulations obtained with the numerical method for non-stiff DDEs for the

Table 2

Values of the parameters in the modified logistic equation. For σ and μ_2 , only the nominal values are shown.

Model, kernel, and simulation parameters									
σ [1/mo]	κ [-]	γ_1 [-]	γ_2 [-]	μ_1 [mo]	μ_2 [mo]	σ_1 [mo]	σ_2 [mo]	t_0 [mo]	t_f [mo]
4	1	0.5	0.5	0.35	0.45	0.06	0.12	0	24

parameter values indicated in the second row (the colors match). We use a memory horizon of $\Delta t_h = t_f - t_0 = 24$ mo and 10,000 time steps. In both cases, the stability analysis based on the approximate set of ODEs (4.7) accurately predicts when the steady state is stable, marginally stable (where the largest real part of the eigenvalues is equal to zero), and unstable. For large values of σ , a limit cycle appears whereas for large values of μ_2 , the population density oscillates unstably. Figure 5 shows the identified kernels, the corresponding error, and the coefficients for different values of μ_2 . In the left column, the coefficients exhibit oscillation, whereas in the right column, there is a similarity between the coefficients and the shape of the approximated kernel, e.g., in terms of bimodality. The oscillations in the coefficients disappear for larger values of M , which also leads to larger values of a (results not shown).

7.2. Nuclear fission. Next, we consider a point reactor kinetics model of a molten salt nuclear fission reactor [15, 53] where the molten salt is circulated through a heat exchanger outside of the reactor core. The model describes 1) the concentrations of $N_g = 6 \in \mathbb{N}$ neutron precursor groups, $C_i : \mathbb{R} \rightarrow \mathbb{R}_{\geq 0}$ for $i = 1, \dots, N_g$, which emit delayed neutrons, 2) the concentration of neutrons, $C_n : \mathbb{R} \rightarrow \mathbb{R}_{\geq 0}$ for $n = N_g + 1 \in \mathbb{N}$, and 3) the reactivity, $\rho : \mathbb{R} \rightarrow \mathbb{R}$, which represents the relative number of neutrons created per fission event:

$$(7.3) \quad \dot{C}_i(t) = (C_{i,in}(t) - C_i(t))D + R_i(t), \quad \dot{C}_n(t) = R_n(t), \quad \dot{\rho}(t) = -\kappa H C_n(t).$$

The dilution rate, $D \in \mathbb{R}_{\geq 0}$, is the ratio between the volumetric inlet and outlet flow rate and the reactor core volume, $\kappa \in \mathbb{R}_{\geq 0}$ is a proportionality constant, and $H \in \mathbb{R}_{\geq 0}$ is the ratio between the power production proportionality constant and the heat capacity of the reactor core. Furthermore, the production rate $R : \mathbb{R} \rightarrow \mathbb{R}^n$ is defined in terms of the stoichiometric matrix $S \in \mathbb{R}^{N_r \times n}$ where $N_r = n \in \mathbb{N}$ is the number of reactions and $r : \mathbb{R} \rightarrow \mathbb{R}_{\geq 0}^{N_r}$ is a vector of reaction rates:

$$(7.4) \quad R(t) = S^T(t)r(t), \quad S(t) = \begin{bmatrix} -1 & & & 1 \\ & \ddots & & \vdots \\ & & -1 & 1 \\ \beta_1 & \cdots & \beta_{N_g} & \rho(t) - \beta \end{bmatrix}, \quad r(t) = \begin{bmatrix} \lambda_1 C_1(t) \\ \vdots \\ \lambda_{N_g} C_{N_g}(t) \\ C_n(t)/\Lambda \end{bmatrix}.$$

Here, $\lambda_i, \beta_i, \Lambda \in \mathbb{R}_{\geq 0}$ for $i = 1, \dots, N_g$ are decay constants, delayed neutron fractions (i.e., the relative number of neutrons that are generated from the decay of neutron precursors), and the mean neutron generation time, respectively, and $\beta \in \mathbb{R}_{\geq 0}$ is the sum of β_i for $i = 1, \dots, N_g$. The inlet concentration, $C_{i,in} : \mathbb{R} \rightarrow \mathbb{R}_{\geq 0}$, is the memory state given by

$$(7.5) \quad C_{i,in}(t) = \int_{-\infty}^t \alpha_i(t-s)C_i(s) ds, \quad i = 1, \dots, N_g.$$

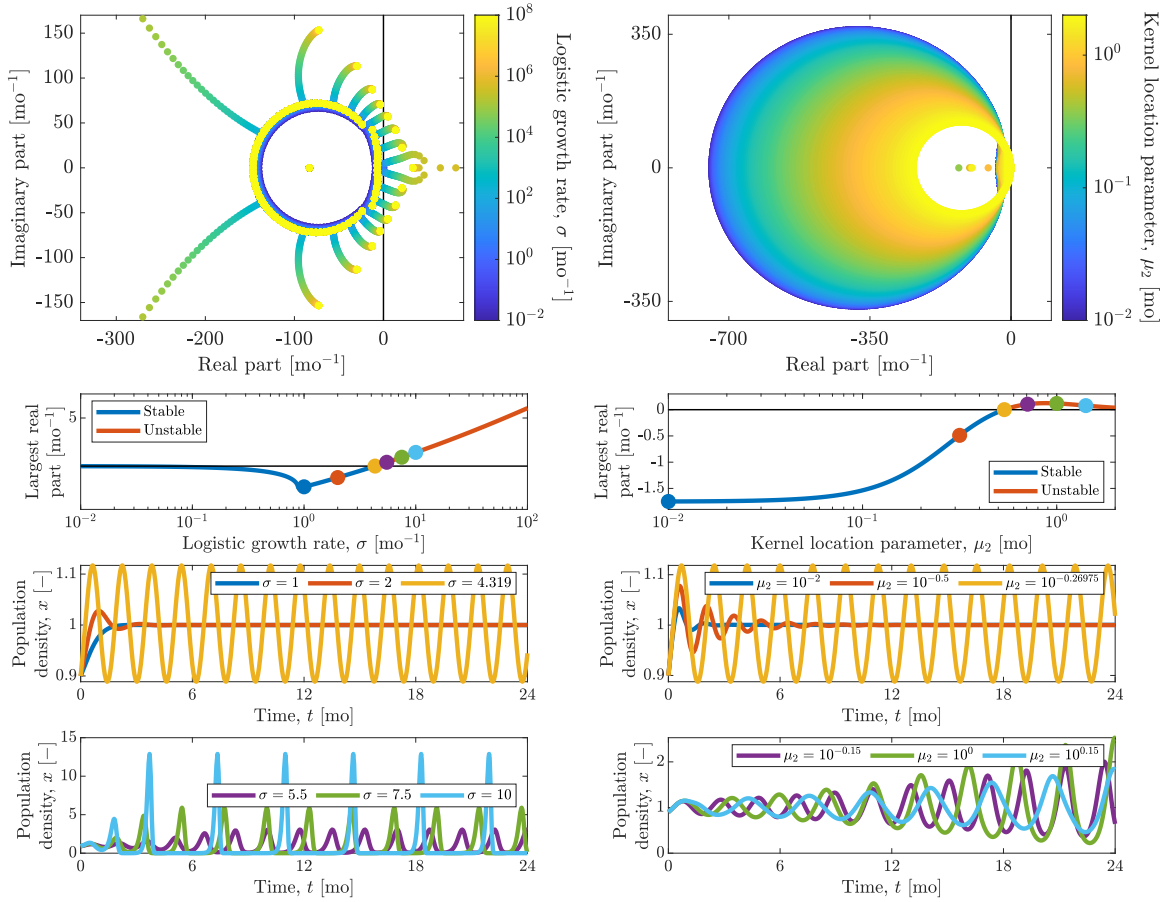


Figure 4. Bifurcation analysis with respect to the model parameter σ (left column) and the kernel parameter μ_2 (right column) for the modified logistic equation. First row: Eigenvalues. Second row: The largest real part of the eigenvalues. Third and bottom row: Simulations for selected parameter values (obtained with the numerical method described in Appendix G.1).

The kernels are described in Appendix H and represent 1) a nonuniform velocity profile in the external circulation of the molten salt (and neutron precursors) and 2) the (exponential) decay of the neutron precursors during the external circulation.

Table 3 shows the parameter values, which (except for D , μ_1 , and σ_1) are taken from [34]. We use $N = 1000$ points to identify Erlang mixture kernel approximations of order $M = 500$. Furthermore, we use $\epsilon = 10^{-13}$ and a tolerance of 10^{-14} in the bisection algorithm (see Table 1), we use Matlab's `integral` with absolute and relative tolerances of 10^{-15} to approximate β in (3.3). Figure 6 shows a Monte Carlo simulation for 1000 samples of κ drawn from a normal distribution with mean $3 \cdot 10^{-4}$ and standard deviation $7.5 \cdot 10^{-5}$. For brevity of the presentation, we omit the plots of the neutron precursor group concentrations. The initial states are $C_i(t) = 1 \text{ kmol/cm}^3$ for $i = 1, \dots, n$ and $\rho(t) = 1.1\beta$ for $t \leq t_0$, and we use an absolute and relative tolerance of 10^{-8} in `ode15s` to simulate the approximate system of ODEs (4.7). Furthermore, we supply the analytical Jacobian of the right-hand side function,

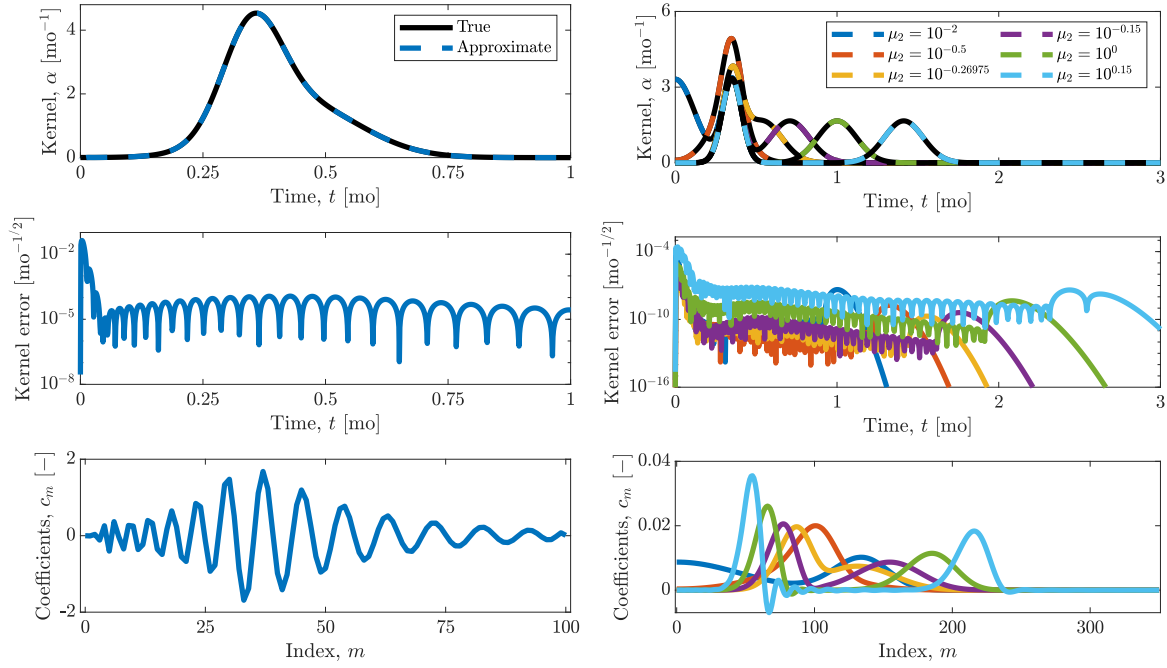


Figure 5. Top row: The true kernels and the corresponding Erlang mixture approximations for $M = 100$ (left) and $M = 350$ (right) obtained in connection with the bifurcation analysis shown in Figure 4. Middle row: The absolute errors of the kernel approximations. Bottom row: The coefficients in the Erlang mixture approximations. The colors are consistent across each column, and the coefficients are visualized as solid lines to ease the interpretation of the results.

Table 3

Values of the parameters in the molten salt reactor model. For κ , only the nominal value is shown.

Decay constants [1/s]					
λ_1	λ_2	λ_3	λ_4	λ_5	λ_6
0.0124	0.0305	0.1110	0.3010	1.1300	3.0000
Delayed neutron fractions [-]					
β_1	β_2	β_3	β_4	β_5	β_6
0.00021	0.00141	0.00127	0.00255	0.00074	0.00027
Other model parameters					
Λ [s]	κ [1/K]	H [K cm ³ /s]	D [1/s]	μ_1 [s]	σ_1 [s]
$5 \cdot 10^{-5}$	$3 \cdot 10^{-4}$	0.05	2	2	0.1

and we represent it as a sparse matrix. The figure also shows the relative difference between the simulations obtained 1) as described above and 2) with the numerical method for stiff DDEs described in Appendix G.2 for the mean value of κ . The latter method uses a time step size of $6.25 \cdot 10^{-5}$ s, and the relative difference, $E_{r,i} : \mathbb{R} \rightarrow \mathbb{R}_{\geq 0}$, in the i 'th state variable and

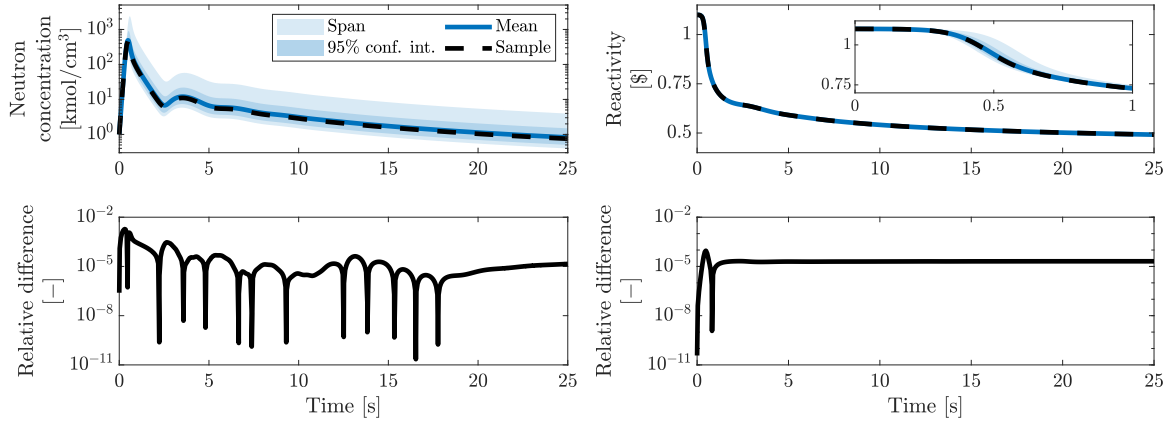


Figure 6. Monte Carlo simulation of the molten salt reactor model. Top row: The neutron concentration (left) and the reactivity (right). For each point in time, the span shows the interval of the minimum and maximum state, and the 95% confidence interval spans the 2.5 and 97.5 percentiles. The mean is computed pointwise, and the sample is the simulation corresponding to the mean value of κ . Bottom row: The pointwise relative error (7.6) between simulating the approximate ODEs (4.7) using `ode15s` and simulating the original DDEs using the numerical method for stiff DDEs described in Appendix G.2.

n 'th time step is given by

$$(7.6) \quad E_{r,i}(t_n) = \frac{|\hat{x}_i(t_n) - x_i(t_n)|}{1 + |x_i(t_n)|}, \quad i = 1, \dots, n_x,$$

where \hat{x}_i is the approximate solution to the ODEs (4.7) and x_i is obtained with the numerical method for stiff DDEs. For each point in time, the 95% confidence intervals show the intervals from the 2.5 to the 97.5 percentiles and the span shows the interval of the minimum and maximum value of the states. For the neutron concentration, the confidence interval is almost symmetric (on the logarithmic axis) whereas the maximum is significantly higher above the mean than the minimum is below it. For the reactivity, the confidence interval and the span are hardly visible, and the simulation for the mean value of κ is indistinguishable from the pointwise mean. The maximum relative difference for all eight state variables is $2.14 \cdot 10^{-3}$. There are three main sources of error that affect this difference: 1) The kernel approximation error, 2) the error from using `ode15s` to simulate the approximate set of ODEs, and 3) the error of the numerical method described in Appendix G.2. If we use twice as large time steps in the latter, the maximum relative error is $4.28 \cdot 10^{-3}$, i.e., twice as large (results not shown). Therefore, we believe that the maximum relative difference would be further reduced by using smaller time step sizes, i.e., that the main source of error is that of the numerical method for stiff DDEs and not the Erlang mixture kernel approximation. However, due to large memory requirements, it has not been possible to further reduce the time step size. Finally, Figure 7 shows the Erlang mixture approximations of the kernels and the corresponding errors. It also shows the sum of folded normal kernels in (H.1) for the values of μ_1 and σ_1 shown in Table 3 and the coefficients in the Erlang mixture approximations. The coefficients exhibit oscillations, which was also the case for the coefficients in the left column of Figure 5.

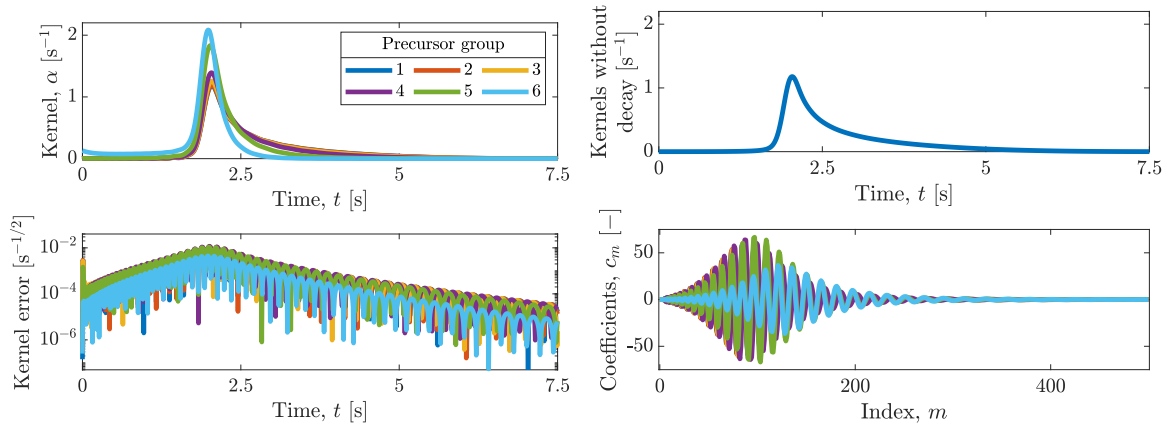


Figure 7. Left column: The Erlang mixture approximations of the kernels in (H.1) used in the Monte Carlo simulation shown in Figure 6 (top) and the corresponding approximation errors (bottom). Right column: The normalized sum of folded normal kernels in the expression (H.1) without the decay factor (top) and the coefficients in the Erlang mixture kernel approximations. The colors are consistent across all but the top right figure.

8. Conclusions. In this paper, we propose an approximate approach for simulating and analyzing DDEs with distributed time delays based on conventional methods for ODEs. Specifically, we approximate the involved kernel by an Erlang mixture kernel and transform the resulting DDEs to ODEs using the LCT. We prove that if the kernel α is regular (Definition 3.2) and the coefficients are chosen as in (4.3), then an Erlang mixture approximation, $\hat{\alpha}$, of order M converges pointwise to α and the integral of the absolute error converges to zero as the rate parameter, a , and the order, M , go to infinity provided that the ratio M/a goes to infinite as well (Proposition 4.2). The main theoretical result of the paper is Theorem 4.4, which states that 1) accurate stability analyses of the steady states of the original system of DDEs (3.1b)–(3.2) can be performed based on the approximate system of ODEs (4.7) if the kernel α is also exponentially bounded, and 2) the solution to the approximate ODEs converges uniformly to that of the original system. Additionally, we propose an approach for determining optimal Erlang mixture approximations based on bisection and least-squares estimation, and we use numerical examples to demonstrate that its accuracy and rate of convergence can be higher than using the theoretical expressions for the coefficients in (4.3). We also compare with the accuracy of an exponential mixture approximation from the literature. Finally, we present two numerical examples that demonstrate the efficacy of the proposed approach, and we compare the results with those obtained by two numerical methods (for non-stiff and stiff systems) formulated directly for DDEs with distributed time delays.

Future work may involve the derivation of error bounds, an extension to Erlang mixture approximations with multiple rate parameters, and an extension to systems with time-varying kernels.

Acknowledgments. The author would like to acknowledge many inspiring discussions on distributed time delays and delay differential equations with Prof. John Wyller from the Norwegian University of Life Sciences, Norway. The author would also like to thank Jonas

Lolle Björnsson for fruitful discussions on Erlang mixture approximations. Finally, the author would like to thank the reviewers for their efforts to improve the generality of the theory presented in the paper.

REFERENCES

- [1] I. AL-DARABSAH, S. A. CAMPBELL, AND B. RAHMAN, *Distributed delay and desynchronization in a neural mass model*, SIAM Journal on Applied Dynamical Systems, 23 (2024), pp. 3013–3051, <https://doi.org/10.1137/23M1618028>.
- [2] A. ALEKSANDROV, D. EFIMOV, AND E. FRIDMAN, *Analysis of homogeneous systems with distributed delay using averaging approach*, IFAC PapersOnLine, 56 (2023), pp. 174–179, <https://doi.org/10.1016/j.ifacol.2023.10.1565>.
- [3] A. ALEKSANDROV, D. EFIMOV, AND E. FRIDMAN, *On stability of nonlinear homogeneous systems with distributed delays having variable kernels*, Systems and Control Letters, 190 (2024), p. 105853, <https://doi.org/10.1016/j.sysconle.2024.105853>.
- [4] O. BAZIGHIFAN, E. M. ELABBASY, AND O. MOAAZ, *Oscillation of higher-order differential equations with distributed delay*, Journal of Inequalities and Applications, 2019 (2019), <https://doi.org/10.1186/s13660-019-2003-0>.
- [5] A. BELLEN, *Numerical methods for delay differential equations: Accuracy and stability problems*, IFAC Proceedings Volumes, 33 (2000), pp. 127–128, [https://doi.org/10.1016/S1474-6670\(17\)36928-8](https://doi.org/10.1016/S1474-6670(17)36928-8).
- [6] H. BERGLAND, P. MISHRA, P. A. PEDERSEN, A. PONOSSOV, AND J. WYLLER, *Time delays and pollution in an open-access fishery*, Natural Resource Modeling, 36 (2022), p. e12363, <https://doi.org/10.1111/nrm.12363>.
- [7] T. CASSIDY, *Distributed delay differential equation representations of cyclic differential equations*, SIAM Journal of Applied Mathematics, 81 (2021), pp. 1742–1766, <https://doi.org/10.1137/20M1351606>.
- [8] T. CASSIDY, M. CRAIG, AND A. R. HUMPHRIES, *Equivalences between age structured models and state dependent distributed delay differential equations*, Mathematical Biosciences and Engineering, 16 (2019), pp. 5419–5450, <https://doi.org/10.3934/mbe.2019270>.
- [9] T. CASSIDY, P. GILLICH, A. R. HUMPHRIES, AND C. H. VAN DORP, *Numerical methods and hypoexponential approximations for gamma distributed delay differential equations*, IMA Journal of Applied Mathematics, 87 (2022), pp. 1043–1089, <https://doi.org/10.1093/imamat/hxac027>.
- [10] O. CHRISTENSEN AND K. L. CHRISTENSEN, *Approximation theory: From Taylor polynomials to wavelets*, Applied and Numerical Harmonic Analysis, Springer, 2005.
- [11] O. DIEKMANN AND M. GYLLENBERG, *Equations with infinite delay: Blending the abstract and the concrete*, Journal of Differential Equations, 252 (2012), pp. 819–851, <https://doi.org/10.1016/j.jde.2011.09.038>.
- [12] O. DIEKMANN, M. GYLLENBERG, AND J. A. J. METZ, *Finite dimensional state representation of linear and nonlinear delay systems*, Journal of Dynamics and Differential Equations, 30 (2018), pp. 1439–1467, <https://doi.org/10.1007/s10884-017-9611-5>.
- [13] O. DIEKMANN, M. GYLLENBERG, AND J. A. J. METZ, *Finite dimensional state representation of physiologically structured populations*, Journal of Mathematical Biology, 80 (2020), pp. 205–273, <https://doi.org/10.1007/s00285-019-01454-0>.
- [14] DTU COMPUTING CENTER, *DTU Computing Center resources*, 2025, <https://doi.org/10.48714/DTU.HPC.0001>.
- [15] J. J. DUDERSTADT AND L. J. HAMILTON, *Nuclear reactor analysis*, Wiley, 1976.
- [16] A. S. EREMIN, *Runge-Kutta methods for differential equations with distributed delays*, AIP Conference Proceedings, 2116 (2019), p. 140003, <https://doi.org/10.1063/1.5114130>.
- [17] L. GUERRINI, A. KRAWIEC, AND M. SZYDŁOWSKI, *Bifurcations in an economic growth model with a distributed time delay transformed to ODE*, Nonlinear Dynamics, 101 (2020), pp. 1263–1279, <https://doi.org/10.1007/s11071-020-05824-y>.
- [18] N. GUGLIELMI AND E. HAIRER, *Applying stiff integrators for ordinary differential equations and delay differential equations to problems with distributed delays*, SIAM Journal on Scientific Computing, 47

- (2025), pp. A102–A123, <https://doi.org/10.1137/24M1632413>.
- [19] L.-S. HAHN AND B. EPSTEIN, *Classical complex analysis*, Jones and Bartlett Books in Mathematics and Computer Science, Jones and Bartlett, 1996.
- [20] J. K. HALE AND S. M. V. LUNEL, *Introduction to functional differential equations*, vol. 99 of Applied Mathematical Sciences, Springer, 1993, <https://doi.org/10.1007/978-1-4612-4342-7>.
- [21] R. A. HORN AND C. R. JOHNSON, *Topics in matrix analysis*, Cambridge University Press, 1991, <https://doi.org/10.1017/CBO9780511840371>.
- [22] R. A. HORN AND C. R. JOHNSON, *Matrix Analysis*, Cambridge University Press, 2nd ed., 2012, <https://doi.org/10.1017/CBO9781139020411>.
- [23] S. HU, M. DUNLAVEY, S. GUZY, AND N. TEUSCHER, *A distributed delay approach for modeling delayed outcomes in pharmacokinetics and pharmacodynamics studies*, *Journal of Pharmacokinetics and Pharmacodynamics*, 45 (2018), pp. 285–308, <https://doi.org/10.1007/s10928-018-9570-4>.
- [24] C. HUANG AND S. VANDEWALLE, *An analysis of delay-dependent stability for ordinary and partial differential equations with fixed and distributed delays*, *SIAM Journal on Scientific Computing*, 25 (2004), pp. 1608–1632, <https://doi.org/10.1137/S1064827502409717>.
- [25] P. J. HURTADO AND A. S. KIROSINGH, *Generalizations of the ‘Linear Chain Trick’: Incorporating more flexible dwell time distributions into mean field ODE models*, *Journal of Mathematical Biology*, 79 (2019), pp. 1831–1883, <https://doi.org/10.1007/s00285-019-01412-w>.
- [26] P. J. HURTADO AND C. RICHARDS, *A procedure for deriving new ODE models: Using the generalized linear chain trick to incorporate phase-type distributed delay and dwell time assumptions*, *Mathematics in Applied Sciences and Engineering*, 1 (2020), pp. 412–424, <https://doi.org/10.5206/mase/10857>.
- [27] P. J. HURTADO AND C. RICHARDS, *Building mean field ODE models using the generalized linear chain trick & Markov chain theory*, *Journal of Biological Dynamics*, 15 (2021), pp. S248–S272, <https://doi.org/10.1080/17513758.2021.1912418>.
- [28] O. C. IBE, *Fundamentals of applied probability and random processes*, Elsevier, 2nd ed., 2014, <https://doi.org/10.1016/C2013-0-19171-4>.
- [29] O. KALLENBERG, *Foundations of modern probability*, Springer, 2002, <https://doi.org/10.1007/978-3-030-61871-1>.
- [30] V. KOLMANOVSKII AND A. MYSHKIS, *Applied theory of functional differential equations*, vol. 85 of Mathematics and Its Applications, Springer, 1992, <https://doi.org/10.1007/978-94-015-8084-7>.
- [31] J. KOREVAAR, *Mathematical methods*, vol. 1, Academic Press, 1968.
- [32] W. KRZYZANSKI, *Ordinary differential equation approximation of gamma distributed delay model*, *Journal of Pharmacokinetics and Pharmacodynamics*, 46 (2019), pp. 53–63, <https://doi.org/10.1007/s10928-018-09618-z>.
- [33] W. KRZYZANSKI, S. HU, AND M. DUNLAVEY, *Evaluation of performance of distributed delay model for chemotherapy-induced myelosuppression*, *Journal of Pharmacokinetics and Pharmacodynamics*, 45 (2018), pp. 329–337, <https://doi.org/10.1007/s10928-018-9575-z>.
- [34] S. Q. B. LEITE, M. T. DE VILHENA, AND B. E. J. BODMANN, *Solution of the point reactor kinetics equations with temperature feedback by the ITS2 method*, *Progress in Nuclear Energy*, 91 (2016), pp. 240–249, <https://doi.org/10.1016/j.pnucene.2016.05.001>.
- [35] N. MACDONALD, *Time lags in biological models*, vol. 27 of Lecture Notes in Biomathematics, Springer, 1978, <https://doi.org/10.1007/978-3-642-93107-9>.
- [36] D. H. NEVERMANN AND C. GROS, *Mapping dynamical systems with distributed time delays to sets of ordinary differential equations*, *Journal of Physics A: Mathematical and Theoretical*, 56 (2023), p. 345702, <https://doi.org/10.1088/1751-8121/acea06>.
- [37] S.-I. NICULESCU AND K. GU, eds., *Advances in time-delay systems*, vol. 38 of Lecture Notes in Computational Science and Engineering, Springer, 2004, <https://doi.org/10.1007/978-3-642-18482-6>.
- [38] J. NOCEDAL AND S. J. WRIGHT, *Numerical optimization*, Springer Series in Operations Research and Financial Engineering, Springer, 2nd ed., 2006, <https://doi.org/10.1007/978-0-387-40065-5>.
- [39] A. D. POLYANIN, V. G. SOROKIN, AND A. I. ZHUROV, *Delay ordinary and partial differential equations*, *Advances in Applied Mathematics*, CRC Press, 2023, <https://doi.org/10.1201/9781003042310>.
- [40] A. PONOSOV, A. SHINDIAPIN, AND J. J. MIGUEL, *The W-transform links delay and ordinary differential equations*, *Functional Differential Equations*, 9 (2002), pp. 437–469.
- [41] M. H. PROTTER AND C. B. MORREY, JR., *Intermediate Calculus*, Undergraduate Texts in Mathematics,

- Springer, 2nd ed., 1985, <https://doi.org/10.1007/978-1-4612-1086-3>.
- [42] B. RAHMAN, K. B. BLYUSS, AND Y. N. KYRYCHKO, *Dynamics of neural systems with discrete and distributed time delays*, SIAM Journal on Applied Dynamical Systems, 14 (2015), pp. 2069–2095, <https://doi.org/10.1137/15M1006398>.
- [43] T. K. S. RITSCHHEL, *Numerical optimal control for distributed delay differential equations: A simultaneous approach based on linearization of the delayed variables*, in Proceedings of the 23rd European Control Conference (ECC'25), 2025, <https://arxiv.org/abs/2410.15083>. Accepted.
- [44] T. K. S. RITSCHHEL AND J. WYLLER, *An algorithm for distributed time delay identification without a priori knowledge of the kernel*, Automatica, 178 (2025), p. 112382, <https://doi.org/10.1016/j.automatica.2025.112382>.
- [45] P. J. ROACHE, *Code verification by the method of manufactured solutions*, Journal of Fluids Engineering, 124 (2002), pp. 4–10, <https://doi.org/10.1115/1.1436090>.
- [46] D. ROMIK, *Stirling's approximation for $n!$: The ultimate short proof?*, The American Mathematical Monthly, 107 (2000), pp. 556–557, <https://doi.org/10.1080/00029890.2000.12005235>.
- [47] H. L. ROYDEN AND P. M. FITZPATRICK, *Real analysis*, Pearson, 4th ed., 2010.
- [48] W. RUDIN, *Principles of mathematical analysis*, International Series in Pure and Applied Mathematics, McGraw-Hill, 3rd ed., 1976.
- [49] L. F. SHAMPINE AND S. THOMPSON, *Solving DDEs in MATLAB*, Applied Numerical Mathematics, 37 (2001), pp. 441–458, [https://doi.org/10.1016/S0168-9274\(00\)00055-6](https://doi.org/10.1016/S0168-9274(00)00055-6).
- [50] H. SMITH, *An introduction to delay differential equations with applications to the life sciences*, vol. 57 of Texts in Applied Mathematics, Springer, 2011, <https://doi.org/10.1007/978-1-4419-7646-8>.
- [51] S. TORKAMANI, E. A. BUTCHER, AND F. A. KHASAWNEH, *Parameter identification in periodic delay differential equations with distributed delay*, Communications in Nonlinear Science and Numerical Simulation, 18 (2013), pp. 1016–1026, <https://doi.org/10.1016/j.cnsns.2012.09.001>.
- [52] Y. WANG, Y. CONG, AND G. HU, *Delay-dependent stability of linear multistep methods for differential systems with distributed delays*, Applied Mathematics and Mechanics, 39 (2018), pp. 1837–1844, <https://doi.org/10.1007/s10483-018-2392-9>.
- [53] D. WOOTEN AND J. J. POWERS, *A review of molten salt reactor kinetics models*, Nuclear Science and Engineering, 191 (2018), pp. 203–230, <https://doi.org/10.1080/00295639.2018.1480182>.
- [54] X. YAN, R. BAUER, G. KOCH, J. SCHROPP, J. J. P. RUIXO, AND W. KRZYZANSKI, *Delay differential equations based models in NONMEM*, Journal of Pharmacokinetics and Pharmacodynamics, 48 (2021), pp. 763–802, <https://doi.org/10.1007/s10928-021-09770-z>.
- [55] Y. YUAN AND J. BÉLAIR, *Stability and Hopf bifurcation analysis for functional differential equation with distributed delay*, SIAM Journal on Applied Dynamical Systems, 10 (2011), pp. 551–581, <https://doi.org/10.1137/100794493>.
- [56] F. ZHANG, *The Schur complement and its applications*, vol. 4 of Numerical Methods and Algorithms, Springer, 2005, <https://doi.org/10.1007/b105056>.
- [57] G. ZHANG AND A. XIAO, *Exact and numerical stability analysis of reaction-diffusion equations with distributed delays*, Frontiers of Mathematics in China, 11 (2016), pp. 189–205, <https://doi.org/10.1007/s11464-015-0506-7>.
- [58] Z. ZHOU, *Statistical inference of distributed delay differential equations*, PhD thesis, University of Iowa, 2016, <https://doi.org/10.17077/etd.xgcf76n>.

Appendix A. Convergence of Taylor polynomial of exponential function. In this appendix, we show a result that involves a truncation of the sum in (2.2), which is used in many of the proofs in this work.

Lemma A.1. *For any $t \in \mathbb{R}_{\geq 0}$, the following expression converges to one as $a \rightarrow \infty$ if $M/a \rightarrow \infty$ as well:*

$$(A.1) \quad e^{-at} \sum_{m=0}^M \frac{(at)^m}{m!} \rightarrow 1.$$

Proof. We use the bound on the error of the Taylor polynomial of e^{at} around $t = 0$ (see, e.g., [10, Thm. 1.3.6 and its proof]):

$$(A.2) \quad \left| 1 - e^{-at} \sum_{m=0}^M \frac{(at)^m}{m!} \right| = e^{-at} \left| e^{at} - \sum_{m=0}^M \frac{(at)^m}{m!} \right| \leq e^{-at} e^{at} \frac{(at)^{M+1}}{(M+1)!} = \frac{(at)^{M+1}}{(M+1)!}$$

Next, we show that this bound converges to zero if $M/a \rightarrow \infty$. Specifically, we show that its logarithm converges to $-\infty$:

$$(A.3) \quad \begin{aligned} \ln \frac{(at)^{M+1}}{(M+1)!} &= (M+1) \ln at - \ln(M+1)! \\ &\approx (M+1) \ln at - \left((M+1) \ln(M+1) - (M+1) + \frac{1}{2} \ln 2\pi(M+1) \right) \\ &\leq (M+1) (\ln at - \ln(M+1) + 1) = (M+1) \left(\ln \frac{a}{M+1} + \ln t + 1 \right). \end{aligned}$$

We have used Stirling's approximation (see Section 2) of $\ln(M+1)!$, and the last expression converges to $-\infty$ if $a/(M+1) \rightarrow 0$ or, equivalently, if $(M+1)/a \rightarrow \infty$. Note that the error of Stirling's approximation converges to zero as $M \rightarrow \infty$, i.e., the result will also hold even though Stirling's approximation was used. \blacksquare

Appendix B. Erlang mixture delta family. In this appendix, we introduce the Erlang mixture delta family and use it to derive an identity for Erlang mixture kernels, which is used to prove uniform convergence of Erlang mixture approximations in Section 4.1. For a given rate parameter, a , the identity also provides the theoretical expressions for the coefficients in (4.3), which depend on the kernel α that is being approximated. Furthermore, we prove a number of statements about the delta family that will also be used in Section 4.1. Throughout this appendix, the time argument t is a fixed parameter.

Lemma B.1 (Erlang mixture delta family). *Let $\delta_a : \mathbb{R}_{\geq 0} \times \mathbb{R}_{\geq 0} \rightarrow \mathbb{R}_{\geq 0}$ be an Erlang mixture delta family of order $M \in \mathbb{N}_{\geq 0}$ with rate parameter $a \in \mathbb{R}_{> 0}$ defined as the piecewise constant function*

$$(B.1) \quad \delta_a(t, s) = \begin{cases} \ell_0(t), & s \in [s_0, s_1), \\ \vdots & \\ \ell_M(t), & s \in [s_M, s_{M+1}), \\ 0, & s \in [s_{M+1}, \infty), \end{cases}$$

where ℓ_m is an Erlang kernel of m 'th order with rate parameter a . The boundaries of the intervals over which δ_a is constant are $s_m = m\Delta s \in \mathbb{R}_{\geq 0}$ for $m = 0, \dots, M+1$, and the width of the intervals is $\Delta s = s_{m+1} - s_m \in \mathbb{R}_{> 0}$, which depends on a . In each interval, δ_a is equal to an Erlang kernel of different order. Then, the following statement holds.

(a) The Erlang mixture kernel, $\hat{\alpha} : \mathbb{R}_{\geq 0} \rightarrow \mathbb{R}$, defined in (4.3) satisfies the identity

$$(B.2) \quad \hat{\alpha}(t) = \int_0^\infty \delta_a(t, s) \alpha(s) ds.$$

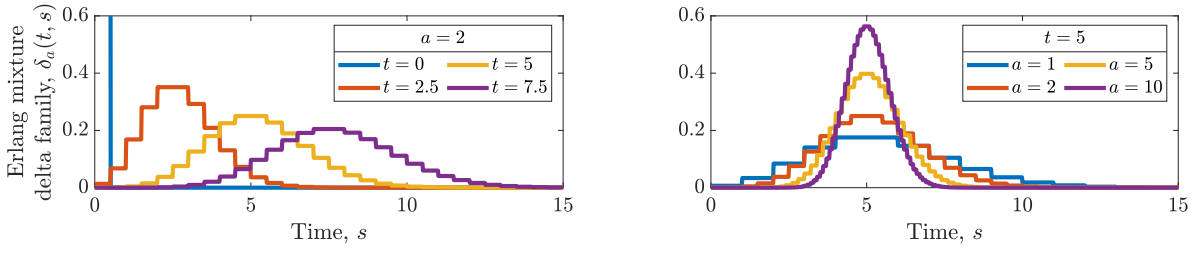


Figure 8. An infinite-order Erlang mixture delta family for a fixed rate parameter, a , and different values of t (left) and for fixed t and different values of a (right). For $t = 0$ in the left figure, the value of δ_a is 2 for $s \in [0, 0.5)$ (see also Corollary B.2).

Furthermore, the following asymptotic properties hold as $a \rightarrow \infty$ when $M/a \rightarrow \infty$ as well.

(b) The integral of δ_a over the second argument converges to one from below, i.e.,

$$(B.3) \quad \int_0^\infty \delta_a(t, s) ds \rightarrow 1, \quad \int_0^\infty \delta_a(t, s) ds \leq 1.$$

(c) For any $\gamma \in \mathbb{R}_{>0}$, $\delta_a(t, s)$ converges uniformly to zero for all $s \in \mathbb{R}_{\geq 0}$ satisfying $\gamma \leq |t - s| < \infty$:

$$(B.4) \quad \delta_a(t, s) \rightarrow 0.$$

(d) For all $\gamma \in \mathbb{R}_{>0}$ and $t \in \mathbb{R}_{\geq 0}$,

$$(B.5) \quad \int_{[t-\gamma]^+}^{t+\gamma} \delta_a(t, s) ds \rightarrow 1.$$

Corollary B.2. For $t = 0$, the Erlang mixture delta family is given by

$$(B.6) \quad \delta_a(0, s) = \begin{cases} a, & s \in [0, 1/a), \\ 0, & \text{otherwise.} \end{cases}$$

Proof. By direct substitution, $\ell_0(0) = a$ and $\ell_m(0) = 0$ for $m > 0$. Furthermore, by definition, $[s_0, s_1) = [0, 1/a)$. ■

Proof of Lemma B.1(a). The identity follows directly from the substitution of the definition of the Erlang mixture delta family in (B.1):

$$(B.7) \quad \int_0^\infty \delta_a(t, s) \alpha(s) ds = \sum_{m=0}^M \ell_m(t) \int_{s_m}^{s_{m+1}} \alpha(s) ds.$$

When the coefficients, $\{c_m\}_{m=0}^M$, are defined as in (4.3), the expression on the right-hand side is equal to the Erlang mixture kernel, $\hat{\alpha}(t)$, in the same equation. ■

Proof of Lemma B.1(b). We substitute the expression for δ_a in (B.1) and simplify:

$$(B.8) \quad \int_0^\infty \delta_a(t, s) ds = \sum_{m=0}^M \ell_m(t) \int_{s_m}^{s_{m+1}} 1 ds = \sum_{m=0}^M \ell_m(t) \Delta s = \sum_{m=0}^M \frac{(at)^m}{m!} a e^{-at} \frac{1}{a} = \sum_{m=0}^M \frac{(at)^m}{m!} e^{-at}.$$

The sum contains a finite number of terms in the expression (2.2) for e^{at} , and all terms are non-negative. Consequently, the expression is less than or equal to one. Furthermore, according to Lemma A.1, it converges to one as $a \rightarrow \infty$ when $M/a \rightarrow \infty$ as well. ■

Lemma B.3. *For a sufficiently large ratio M/a , an Erlang mixture delta family, $\delta_a : \mathbb{R}_{\geq 0} \times \mathbb{R}_{\geq 0} \rightarrow \mathbb{R}_{\geq 0}$ of order $M \in \mathbb{N}_{\geq 0}$ with rate parameter $a \in \mathbb{R}_{> 0}$, is non-decreasing in the second argument, s , when it is below the first argument, t , and non-increasing when it is above. Specifically, since δ_a is piecewise constant over intervals of size Δs , $\delta_a(t, s) \leq \delta_a(t, s + \Delta s)$ for $s < t$, and $\delta_a(t, s) \geq \delta_a(t, s + \Delta s)$ for $s \geq t$.*

Proof. Let $s \in [s_{m-1}, s_m)$. Then, $s + \Delta s \in [s_m, s_{m+1})$, and we derive a condition on m for δ_a to be non-decreasing:

$$(B.9) \quad \delta_a(t, s) \leq \delta_a(t, s + \Delta s).$$

When the ratio M/a is sufficiently large, the left- and right-hand sides are equal to $\ell_{m-1}(t)$ and $\ell_m(t)$, respectively, and we substitute their expressions:

$$(B.10) \quad \frac{(at)^{m-1}}{(m-1)!} a e^{-at} \leq \frac{(at)^m}{m!} a e^{-at}.$$

Most factors cancel out, and we obtain the condition

$$(B.11) \quad m \leq at.$$

This corresponds to $s_m = m\Delta s = m/a \leq t$, and $s < s_m$ by assumption. Consequently, δ_a is non-decreasing in s for $s < t$, and the proof that δ_a is non-increasing in s for $s \geq t$ is analogous. ■

Proof of Lemma B.1(c). In the proof, we will use Stirling's approximation (see Section 2) and that the approximation converges, i.e., asymptotic results for the approximate quantity will also hold for the original quantity. We will show that for given $\epsilon \in \mathbb{R}_{> 0}$ and for fixed s and t , it is possible to choose a sufficiently large that the inequality

$$(B.12) \quad \delta_a(t, s) < \epsilon$$

is satisfied if $s \neq t$. Since $M/a \rightarrow \infty$, $\delta_a(t, s) = \ell_m(t)$ for sufficiently large a , and for simplicity, we assume that a is chosen such that $m = as$ is integer. First, we assume that $t > 0$ and substitute ℓ_m and the value of m :

$$(B.13) \quad \frac{(at)^{as}}{(as)!} a e^{-at} < \epsilon.$$

Next, we take the logarithm on both sides and substitute Stirling's approximation:

$$(B.14a) \quad as \ln at - \ln(as)! + \ln a - at < \ln \epsilon,$$

$$(B.14b) \quad as \ln at - \left(as \ln as - as + \frac{1}{2} \ln 2\pi as \right) + \ln a - at < \ln \epsilon.$$

Finally, we rearrange terms:

$$(B.15) \quad a \left(s \left(\ln \frac{t}{s} + 1 \right) - t \right) + \frac{1}{2} \ln a < \ln \epsilon + \frac{1}{2} \ln 2\pi s.$$

For $s \neq t$, the factor of a in the first term is always negative, and it is always possible to satisfy the bound for sufficiently large a . This follows from the inequality $\ln x \leq x - 1$ for $x > 0$. In contrast, if $s = t$, the factor of a is zero, and the inequality is only satisfied if

$$(B.16) \quad \frac{1}{2} \ln a < \ln \epsilon + \frac{1}{2} \ln 2\pi s \quad \text{or} \quad a < 2\pi s \epsilon^2,$$

i.e., if a is bounded from above. For $t = 0$, $\delta_a(t, s)$ is only nonzero for $s < 1/a$ (see Corollary B.2). Consequently, for a fixed $s \neq t$, it is always possible to choose a large enough that $\delta_a(t, s) = 0$. Finally, the convergence is uniform due to the monotonicity properties shown in Lemma B.3, i.e., for a given $\gamma > 0$, a can be chosen large enough that $\max\{\delta_a(t, [t - \gamma]^+), \delta_a(t, t + \gamma)\} < \epsilon$ and the same will hold for all other values of $s \in \mathbb{R}_{\geq 0}$ satisfying $\gamma \leq |t - s| < \infty$. ■

Proof of Lemma B.1(d). First, we assume that $t > 0$ and bound the integral from above and below using Lemma C.5:

$$(B.17) \quad \frac{1}{k} - \frac{\sigma^2(t)}{\bar{\gamma}^2(t)} \leq \int_{k\mu(t) - \bar{\gamma}(t)}^{k\mu(t) + \bar{\gamma}(t)} \delta_a(t, s) ds \leq \int_{[k\mu(t) - \gamma]^+}^{k\mu(t) + \gamma} \delta_a(t, s) ds \leq \int_0^\infty \delta_a(t, s) ds = \frac{1}{k}.$$

Here, $\bar{\gamma}(t) = \min\{\mu(t), \gamma\}$ such that the limits in the leftmost integral are non-negative, and $k = \left(\int_0^\infty \delta_a(t, s) ds \right)^{-1}$. Consequently, since $\mu(t) \rightarrow t$, $\sigma^2(t) \rightarrow 0$, $k \rightarrow 1$, and $\gamma(t) \rightarrow \min\{t, \gamma\} > 0$ as $a \rightarrow \infty$ and $M/a \rightarrow \infty$ (see Lemma B.1(b) and Lemma C.3–C.4), the integral in (B.5) approaches one. Next, if $t = 0$, the integral in (B.5) is equal to one for all $a \geq 1/\gamma$. ■

Appendix C. Erlang mixture delta family: Mean, variance, and Chebyshev's inequality.

In this appendix, we use results from probability theory to prove bounds that are used in the proof of Lemma B.1(d). We will draw on the analogy of δ_a to the probability density function of a non-negative random variable, e.g., by determining its mean and variance.

Definition C.1. For given $t \in \mathbb{R}_{\geq 0}$, the mean, $\mu : \mathbb{R}_{\geq 0} \rightarrow \mathbb{R}_{\geq 0}$, associated with a delta family, $\delta_a : \mathbb{R}_{\geq 0} \times \mathbb{R}_{\geq 0} \rightarrow \mathbb{R}_{\geq 0}$, is given by the integral

$$(C.1) \quad \mu(t) = \int_0^\infty \delta_a(t, s) s ds.$$

Definition C.2. For given $t \in \mathbb{R}_{\geq 0}$, the variance, $\sigma^2 : \mathbb{R}_{\geq 0} \rightarrow \mathbb{R}_{\geq 0}$, associated with a delta family, $\delta_a : \mathbb{R}_{\geq 0} \times \mathbb{R}_{\geq 0} \rightarrow \mathbb{R}_{\geq 0}$, is given by the integral

$$(C.2) \quad \sigma^2(t) = \int_0^\infty \delta_a(t, s)(s - \mu(t))^2 ds,$$

or, equivalently, by

$$(C.3) \quad \sigma^2(t) = \mu_2(t) - \mu^2(t), \quad \mu_2(t) = \int_0^\infty \delta_a(t, s)s^2 ds,$$

where $\mu : \mathbb{R}_{\geq 0} \rightarrow \mathbb{R}_{\geq 0}$ is the mean given by (C.1).

Lemma C.3. For given $t \in \mathbb{R}_{\geq 0}$, the mean, $\mu : \mathbb{R}_{\geq 0} \rightarrow \mathbb{R}_{\geq 0}$, associated with an Erlang mixture delta family, $\delta_a : \mathbb{R}_{\geq 0} \times \mathbb{R}_{\geq 0} \rightarrow \mathbb{R}_{\geq 0}$, of order $M \in \mathbb{N}_{\geq 0}$ with rate parameter a converges to t ,

$$(C.4) \quad \mu(t) \rightarrow t,$$

as $a \rightarrow \infty$ if $M/a \rightarrow \infty$ as well. Furthermore, for finite $a \in \mathbb{R}_{> 0}$, $\mu(t) > 0$ for all $t \in \mathbb{R}_{\geq 0}$.

Proof. We substitute the definition of δ_a in (B.1):

$$(C.5) \quad \mu(t) = \int_0^\infty \delta_a(t, s)s ds = \sum_{m=0}^M \ell_m(t) \int_{s_m}^{s_{m+1}} s ds.$$

Next, we write out the expression for the integral,

$$(C.6) \quad \int_{s_m}^{s_{m+1}} s ds = \frac{1}{2}(s_{m+1}^2 - s_m^2) = \frac{1}{2}(s_{m+1} - s_m)(s_{m+1} + s_m) = \frac{1}{2}\Delta s((m+1) + m)\Delta s \\ = \frac{2m+1}{2}\Delta s^2,$$

and substitute into (C.5):

$$(C.7) \quad \mu(t) = \sum_{m=0}^M \frac{(at)^m}{m!} a e^{-at} \frac{2m+1}{2} \Delta s^2 = t \sum_{m=1}^M \frac{(at)^{m-1}}{(m-1)!} e^{-at} + \frac{1}{2a} \sum_{m=0}^M \frac{(at)^m}{m!} e^{-at} \rightarrow t$$

as $a \rightarrow \infty$ when $M/a \rightarrow \infty$ as well. Here, we have used that $\Delta s = 1/a$, and Lemma A.1. Specifically, the first term converges to the factor t , and the second term converges to zero because of the factor $1/(2a)$. ■

Lemma C.4. For given $t \in \mathbb{R}_{\geq 0}$, the variance, $\sigma^2 : \mathbb{R}_{\geq 0} \rightarrow \mathbb{R}_{\geq 0}$, associated with an Erlang mixture delta family, $\delta_a : \mathbb{R}_{\geq 0} \times \mathbb{R}_{\geq 0} \rightarrow \mathbb{R}_{\geq 0}$, of order $M \in \mathbb{N}_{\geq 0}$ with rate parameter a converges to zero,

$$(C.8) \quad \sigma^2(t) \rightarrow 0,$$

as $a \rightarrow \infty$ if $M/a \rightarrow \infty$ as well.

Proof. First, we write out the integral in the definition of μ_2 in (C.3):

$$(C.9) \quad \mu_2(t) = \int_0^\infty \delta_a(t, s) s^2 ds = \sum_{m=0}^M \ell_m(t) \int_{s_m}^{s_{m+1}} s^2 ds.$$

Next, we write out the integral of s^2 ,

$$(C.10) \quad \begin{aligned} \int_{s_m}^{s_{m+1}} s^2 ds &= \frac{1}{3}(s_{m+1}^3 - s_m^3) = \frac{1}{3}(s_{m+1} - s_m)(s_{m+1}^2 + s_{m+1}s_m + s_m^2) \\ &= \frac{1}{3}\Delta s((m+1)^2 + (m+1)m + m^2)\Delta s^2 \\ &= \left(m(m-1) + 2m + \frac{1}{3}\right) \Delta s^3, \end{aligned}$$

and substitute it into the right-hand side of (C.9):

$$(C.11) \quad \mu_2(t) = \sum_{m=0}^M \frac{(at)^m}{m!} a e^{-at} \left(m(m-1) + 2m + \frac{1}{3}\right) \Delta s^3.$$

We investigate the convergence of each of the three sums separately:

$$(C.12a) \quad \sum_{m=0}^M \frac{(at)^m}{m!} a e^{-at} m(m-1) \Delta s^3 = t^2 \sum_{m=2}^M \frac{(at)^{m-2}}{(m-2)!} e^{-at} \rightarrow t^2,$$

$$(C.12b) \quad \sum_{m=0}^M \frac{(at)^m}{m!} a e^{-at} 2m \Delta s^3 = 2 \frac{t}{a} \sum_{m=1}^M \frac{(at)^{m-1}}{(m-1)!} e^{-at} \rightarrow 0,$$

$$(C.12c) \quad \sum_{m=0}^M \frac{(at)^m}{m!} a e^{-at} \frac{1}{3} \Delta s^3 = \frac{1}{3a^2} \sum_{m=0}^M \frac{(at)^m}{m!} e^{-at} \rightarrow 0,$$

as $a \rightarrow \infty$ when $M/a \rightarrow \infty$ as well. In all three cases, we have used that $\Delta s = 1/a$ and Lemma A.1. The first term converges to the factor t^2 , and the last two terms convergence to zero because of the factors $2t/a$ and $1/(3a^2)$. Consequently, $\mu_2(t) \rightarrow t^2$, and we use the expression for limit of the mean (C.4) and the definition of σ^2 in (C.3) to conclude the proof:

$$(C.13) \quad \sigma^2(t) = \mu_2(t) - \mu^2(t) \rightarrow t^2 - t^2 = 0.$$

We have used that $\mu^2(t) \rightarrow t^2$ when $\mu(t) \rightarrow t$ because the square is continuous. ■

Lemma C.5. *Let $\delta : \mathbb{R}_{\geq 0} \times \mathbb{R}_{\geq 0} \rightarrow \mathbb{R}_{\geq 0}$ be an Erlang mixture delta family with mean $\mu : \mathbb{R}_{\geq 0} \rightarrow \mathbb{R}_{\geq 0}$, variance $\sigma^2 : \mathbb{R}_{\geq 0} \rightarrow \mathbb{R}_{\geq 0}$, and rate parameter $a \in \mathbb{R}_{> 0}$. Furthermore, let $k = \left(\int_0^\infty \delta_a(t, s) ds\right)^{-1} \in \mathbb{R}_{\geq 0}$. Then, the inequality*

$$(C.14) \quad \frac{1}{k} - \int_{k\mu(t)-\gamma}^{k\mu(t)+\gamma} \delta_a(t, s) ds \leq \frac{\sigma^2(t)}{\gamma^2}$$

holds for all $\gamma \in \mathbb{R}_{> 0}$ that satisfy $\gamma \leq \mu(t)$. Furthermore, $k \geq 1$ and $k \rightarrow 1$ as $a \rightarrow \infty$.

Proof. This follows from Chebyshev's (or Markov's) well-known inequality in probability theory and the fact that $\mu(t) > 0$ for all $t \in \mathbb{R}_{\geq 0}$ and finite rate parameters, $a \in \mathbb{R}_{> 0}$. See, e.g., Lemma 4.1 in the book by Kallenberg [29]. In order to apply Chebyshev's inequality, we derive the mean and variance for the scaled Erlang mixture delta family, $k\delta_a$. The mean is also scaled by k ,

$$(C.15) \quad \int_0^\infty k\delta_a(t, s)s \, ds = k \int_0^\infty \delta_a(t, s)s \, ds = k\mu(t),$$

whereas the variance is not directly proportional to σ^2 :

$$(C.16a) \quad \int_0^\infty k\delta_a(t, s)s^2 \, ds = k \int_0^\infty \delta_a(t, s)s^2 \, ds = k\mu_2(t),$$

$$(C.16b) \quad \int_0^\infty k\delta_a(t, s)(s - k\mu(t))^2 \, ds = k\mu_2(t) - k^2\mu^2(t).$$

However, since $k \geq 1$, $-k^2 \leq -k$ and the variance is bounded by $k\mu_2(t) - k\mu^2(t) = k\sigma^2(t)$. Next, Chebyshev's inequality for $k\delta_a$ is

$$(C.17) \quad 1 - \int_{k\mu(t)-\gamma}^{k\mu(t)+\gamma} k\delta_a(t, s) \, ds \leq \frac{k\mu_2(t) - k^2\mu^2(t)}{\gamma} \leq \frac{k\sigma^2(t)}{\gamma},$$

where we have used the bound on the variance of $k\delta_a$. The inequality (C.14) is obtained by dividing by k . ■

Appendix D. Proof of uniform convergence based on delta families. As the delta family δ_a presented in Appendix B depends on both t and s (and not only their difference), the proof that the Erlang mixture approximation converges uniformly requires an adaptation (Lemma D.1) of the theorem presented in Section 9.3 of Chapter 2 in the book by Korevaar [31] on the convergence of approximations based on delta families.

Lemma D.1. *Let $\delta_a : \mathbb{R}_{\geq 0} \times \mathbb{R}_{\geq 0} \rightarrow \mathbb{R}_{\geq 0}$ be a delta family parametrized by $a \in \mathbb{R}_{> 0}$ which satisfies the following conditions for any given $t \in \mathbb{R}_{\geq 0}$.*

1. For all $\gamma \in \mathbb{R}_{> 0}$,

$$(D.1) \quad \int_{[t-\gamma]^+}^{t+\gamma} \delta_a(t, s) \, ds \rightarrow 1$$

as $a \rightarrow \infty$.

2. For any $\gamma \in \mathbb{R}_{> 0}$, $\delta_a(t, s) \rightarrow 0$ uniformly for $s \in \mathbb{R}_{\geq 0}$ satisfying $\gamma \leq |t - s| < \infty$ as $a \rightarrow \infty$.

3. For all $s \in \mathbb{R}_{\geq 0}$ and $a \in \mathbb{R}_{> 0}$, the delta family is non-negative, i.e., $\delta_a(t, s) \geq 0$.

Furthermore, let $\alpha : \mathbb{R}_{\geq 0} \rightarrow \mathbb{R}$ be a regular kernel. Then, the approximation $\hat{\alpha} : \mathbb{R}_{\geq 0} \rightarrow \mathbb{R}$ given by

$$(D.2) \quad \hat{\alpha}(t) = \int_0^\infty \delta_a(t, s)\alpha(s) \, ds$$

converges uniformly to α for all $t \in \mathbb{R}_{\geq 0}$ as $a \rightarrow \infty$.

Proof. First, we split the integral into two terms:

$$(D.3) \quad \hat{\alpha}(t) = \int_0^\infty \delta_a(t, s) \alpha(s) ds \\ = \underbrace{\int_{[t-\gamma]^+}^{t+\gamma} \delta_a(t, s) \alpha(s) ds}_{\mathcal{I}_1(t)} + \underbrace{\int_0^{[t-\gamma]^+} \delta_a(t, s) \alpha(s) ds + \int_{t+\gamma}^\infty \delta_a(t, s) \alpha(s) ds}_{\mathcal{I}_2(t)}.$$

Next, we add zero to the first term and split the integral:

$$(D.4) \quad \mathcal{I}_1(t) = \underbrace{\alpha(t) \int_{[t-\gamma]^+}^{t+\gamma} \delta_a(t, s) ds}_{\mathcal{I}_3(t)} + \underbrace{\int_{[t-\gamma]^+}^{t+\gamma} \delta_a(t, s) (\alpha(s) - \alpha(t)) ds}_{\mathcal{I}_4(t)}.$$

The absolute value of the second term, $\mathcal{I}_4(t)$, can be bounded through the continuity of α . Specifically, choose γ such that $|\alpha(s) - \alpha(t)| < \epsilon$ for $|s - t| < \gamma$. Then,

$$(D.5) \quad |\mathcal{I}_4(t)| < \int_{[t-\gamma]^+}^{t+\gamma} \delta_a(t, s) |\alpha(s) - \alpha(t)| ds < \epsilon \int_{[t-\gamma]^+}^{t+\gamma} \delta_a(t, s) ds < \epsilon.$$

Next, we prove that the term $\mathcal{I}_2(t) \rightarrow 0$ as $a \rightarrow \infty$. We bound $|\mathcal{I}_2|$ from above by substituting the supremum of δ_a , bounding the integrals, and utilizing the non-negativity of δ_a :

$$(D.6) \quad |\mathcal{I}_2(t)| \leq \int_0^{[t-\gamma]^+} \delta_a(t, s) |\alpha(s)| ds + \int_{t+\gamma}^\infty \delta_a(t, s) |\alpha(s)| ds \leq \rho(\infty) \sup_{\substack{s \in \mathbb{R}_{\geq 0} \\ \gamma \leq |t-s| < \infty}} \delta_a(t, s).$$

Furthermore, we note that by assumption, the supremum of δ_a over values of s outside of an interval around t goes to zero as $a \rightarrow \infty$. We choose a large enough that $|\mathcal{I}_2(t)| < \epsilon$. Additionally, we choose a large enough that

$$(D.7) \quad 1 - \int_{[t-\gamma]^+}^{t+\gamma} \delta_a(t, s) ds < \epsilon.$$

Then,

$$(D.8) \quad |\mathcal{I}_3(t) - \alpha(t)| = |\alpha(t)| \left(1 - \int_{[t-\gamma]^+}^{t+\gamma} \delta_a(t, s) ds \right) < |\alpha(t)| \epsilon,$$

and by utilizing the above bounds, we can choose a sufficiently large that

$$(D.9) \quad \begin{aligned} |\hat{\alpha}(t) - \alpha(t)| &< |\mathcal{I}_1(t) - \alpha(t)| + |\mathcal{I}_2(t)| \\ &< |\mathcal{I}_3(t) - \alpha(t)| + |\mathcal{I}_4(t)| + |\mathcal{I}_2(t)| \\ &< (|\alpha(t)| + 2)\epsilon, \\ &\leq (K + 2)\epsilon \end{aligned}$$

for any $\epsilon \in \mathbb{R}_{>0}$. We have made repeated use of triangle equalities. To summarize, for any $\bar{\epsilon} \in \mathbb{R}_{>0}$, we can choose $\bar{a} \in \mathbb{R}_{>0}$ such that $|\hat{\alpha}(t) - \alpha(t)| < \bar{\epsilon}$ for all $a \geq \bar{a}$ when α is bounded, and the convergence is uniform because the bound is independent of t . \blacksquare

Appendix E. Properties of Erlang mixture kernels. In this appendix, we prove Corollary 4.3 and present lemmas on two other properties of Erlang mixture kernels with coefficients given by (4.3) that will be used either to prove convergence of the integral of the absolute error in Section 4.1 or to prove a relation between the stability analyses of the original system in Section 3 and the approximate system of ODEs presented in Theorem 4.4.

Proof of Corollary 4.3. First, we bound the following exponential¹ for $\rho/a \leq \omega$:

$$(E.1) \quad e^{-\rho s_m} = e^{-\rho m/a} = \left(e^{-\rho/a}\right)^m \leq \left(1 - \frac{1 - e^{-\omega}}{\omega} \frac{\rho}{a}\right)^m = \left(1 - \frac{\bar{\rho}}{a}\right)^m = \left(\frac{a - \bar{\rho}}{a}\right)^m.$$

Next, we substitute the exponential bound in the expression for the coefficients in (4.3):

$$(E.2) \quad |c_m| \leq \int_{s_m}^{s_{m+1}} |\alpha(s)| ds \leq L \int_{s_m}^{s_{m+1}} e^{-\rho s} ds = -\frac{L}{\rho} (e^{-\rho s_{m+1}} - e^{-\rho s_m}) \\ = \frac{L}{\rho} e^{-\rho s_m} (1 - e^{-\rho(s_{m+1} - s_m)}) = \frac{L}{\rho} e^{-\rho s_m} (1 - e^{-\rho \Delta s}) \leq L e^{-\rho s_m} \Delta s = L e^{-\rho s_m} \frac{1}{a} \\ \leq L \left(\frac{a - \bar{\rho}}{a}\right)^m \frac{1}{a}.$$

Here, we have used the bound $1 - e^{-\rho \Delta s} \leq \rho \Delta s$. Next, we substitute this bound into the Erlang mixture kernel:

$$(E.3) \quad |\hat{\alpha}(t)| \leq \sum_{m=0}^M |c_m| \ell_m(t) \leq \sum_{m=0}^M L \left(\frac{a - \bar{\rho}}{a}\right)^m \frac{1}{a} \frac{(at)^m}{m!} a e^{-at} = L \sum_{m=0}^M \frac{((a - \bar{\rho})t)^m}{m!} e^{-at} \\ = L e^{-\bar{\rho}t} \sum_{m=0}^M \frac{((a - \bar{\rho})t)^m}{m!} e^{-(a - \bar{\rho})t} \leq L e^{-\bar{\rho}t} e^{(a - \bar{\rho})t} e^{-(a - \bar{\rho})t} = L e^{-\bar{\rho}t}.$$

Again, we have used the identity (2.2) and that all terms in the sum are positive for sufficiently large a . The bound $1 - e^{-\omega} \leq \omega$ provides the bound $\bar{\rho} \leq \rho$, and using the identity (2.2), we show that $\bar{\rho} \rightarrow \rho$ as $\omega \rightarrow 0$:

$$(E.4) \quad \bar{\rho} = \rho \frac{1 - e^{-\omega}}{\omega} = \rho \frac{1 - \sum_{m=0}^{\infty} \frac{(-\omega)^m}{m!}}{\omega} = \rho \sum_{m=1}^{\infty} \frac{(-\omega)^{m-1}}{m!}.$$

The first term in the sum is one, and all other terms converge to zero as $\omega \rightarrow 0$. ■

Lemma E.1. *If the Erlang mixture kernel $\hat{\alpha} : \mathbb{R}_{\geq 0} \rightarrow \mathbb{R}$ is bounded, it is uniformly integrable, i.e., for all $a \in \mathbb{R}_{> 0}$ and for every $\epsilon \in \mathbb{R}_{> 0}$, there exists a $\Delta t \in \mathbb{R}_{> 0}$ such that if $|t_1 - t_0| < \Delta t$, then,*

$$(E.5) \quad \int_{t_0}^{t_1} |\hat{\alpha}(t)| dt < \epsilon.$$

¹The convexity of decaying exponential functions implies that $e^{-x} \leq 1 - \frac{1 - e^{-\omega}}{\omega} x$ for $x \in [0, \omega]$.

Proof. The uniform integrability follows directly from the boundedness:

$$(E.6) \quad \int_{t_0}^{t_1} |\hat{\alpha}(t)| dt \leq \int_{t_0}^{t_1} K dt = K|t_1 - t_0| < K\Delta t.$$

Here, K is the upper bound on $\hat{\alpha}$, and the bound is satisfied for $\Delta t = \epsilon/K$. ■

Lemma E.2. *Let $\alpha : \mathbb{R}_{\geq 0} \rightarrow \mathbb{R}$ be a regular kernel, and let $\hat{\alpha} : \mathbb{R}_{\geq 0} \rightarrow \mathbb{R}$ be an Erlang mixture approximation of order $M \in \mathbb{N}_{\geq 0}$ given by (4.3) with rate parameter $a \in \mathbb{R}_{> 0}$. Then, $\hat{\alpha}$ is tight [47, Sec. 18.3, p. 376], i.e., for every $\epsilon \in \mathbb{R}_{> 0}$, there exists a $t_0 \in \mathbb{R}_{\geq 0}$ such that*

$$(E.7) \quad \int_{t_0}^{\infty} |\hat{\alpha}(t)| < \epsilon$$

for all $a \in \mathbb{R}$. The result also holds for infinite orders, M .

Proof. In order to prove the statement, we present an approach for choosing t_0 for a given ϵ . First, we bound the expression and split the resulting sum:

$$(E.8) \quad \begin{aligned} \int_{t_0}^{\infty} |\hat{\alpha}(t)| dt &= \int_{t_0}^{\infty} \left| \sum_{m=0}^M c_m \ell_m(t) \right| dt \leq \sum_{m=0}^{\infty} |c_m| \int_{t_0}^{\infty} \ell_m(t) dt \\ &= \sum_{m=0}^{m^*} |c_m| \int_{t_0}^{\infty} \ell_m(t) dt + \sum_{m=m^*+1}^{\infty} |c_m| \int_{t_0}^{\infty} \ell_m(t) dt. \end{aligned}$$

Note that we include infinitely many terms in the first inequality. Next, we bound the second sum:

$$(E.9) \quad \begin{aligned} \sum_{m=m^*+1}^{\infty} |c_m| \int_{t_0}^{\infty} \ell_m(t) dt &\leq \sum_{m=m^*+1}^{\infty} |c_m| = \sum_{m=m^*+1}^{\infty} \left| \int_{s_m}^{s_{m+1}} \alpha(s) ds \right| \\ &\leq \sum_{m=m^*+1}^{\infty} \int_{s_m}^{s_{m+1}} |\alpha(s)| ds = \int_{s_{m^*+1}}^{\infty} |\alpha(s)| ds \\ &= \rho(\infty) - \rho(s_{m^*+1}) = \rho(\infty) - \rho\left(\frac{m^*+1}{a}\right). \end{aligned}$$

For the remainder of the proof, we fix the ratio between m^*+1 and a to γ , i.e., $(m^*+1)/a = \gamma$, and we choose γ large enough that $\rho(\infty) - \rho(\gamma) < \epsilon/2$. In order to bound the first sum in the rightmost expression in (E.8), we write out the integral of the Erlang kernel:

$$(E.10) \quad \begin{aligned} \int_{t_0}^{\infty} \ell_m(t) dt &= 1 - \int_0^{t_0} \ell_m(t) dt = 1 - \left(1 - \sum_{n=0}^m \frac{(at_0)^n}{n!} e^{-at_0} \right) \\ &= \sum_{n=0}^m \frac{(at_0)^n}{n!} e^{-at_0}. \end{aligned}$$

As the order, m , only determines the number of terms and since all terms are non-negative, the integral is monotonically non-decreasing in m . Therefore,

$$(E.11) \quad \int_{t_0}^{\infty} \ell_m(t) dt \leq \int_{t_0}^{\infty} \ell_{m^*}(t) dt$$

for $m \leq m^*$, and we substitute the value of a , which depends on m^* and γ :

$$(E.12) \quad \int_{t_0}^{\infty} \ell_{m^*}(t) dt = \sum_{n=0}^{m^*} \frac{\left(\frac{m^*+1}{\gamma} t_0\right)^n}{n!} e^{-(m^*+1)t_0/\gamma}.$$

For sufficiently large ratios t_0/γ , the exponentially decaying factor will cause the expression to be monotonically decreasing for all values of m^* . Note that the convergence proof in Appendix A would also not hold under the conditions considered here, i.e., the rightmost expression in (A.3) would not approach zero. Consequently, we can bound the expression by substituting $m^* = 0$:

$$(E.13) \quad \int_{t_0}^{\infty} \ell_{m^*}(t) dt \leq e^{-t_0/\gamma}.$$

We use these bounds to derive an upper bound on the first sum in the rightmost expression in (E.8):

$$(E.14) \quad \begin{aligned} \sum_{m=0}^{m^*} |c_m| \int_{t_0}^{\infty} \ell_m(t) dt &\leq \int_{t_0}^{\infty} \ell_{m^*}(t) dt \sum_{m=0}^{m^*} |c_m| \leq e^{-t_0/\gamma} \sum_{m=0}^{m^*} |c_m| \\ &\leq e^{-t_0/\gamma} \rho(s_{m^*+1}) = e^{-t_0/\gamma} \rho\left(\frac{m^*+1}{a}\right) \\ &= e^{-t_0/\gamma} \rho(\gamma). \end{aligned}$$

Finally, we combine the two derived bounds:

$$(E.15) \quad \int_{t_0}^{\infty} |\hat{\alpha}(t)| dt \leq \rho(\infty) - \rho(\gamma) + e^{-t_0/\gamma} \rho(\gamma).$$

To summarize, we first choose γ large enough that $\rho(\infty) - \rho(\gamma) < \epsilon/2$ and then we choose t_0 large enough that $e^{-t_0/\gamma} \rho(\gamma) < \epsilon/2$. As γ is constant for all combinations of m^* and a , the bound holds for all values of the rate parameter, a . Furthermore, the result is independent of the order, M , of the Erlang mixture kernel. This concludes the proof. \blacksquare

Appendix F. Derivation of the linear chain trick. In this appendix, we show the derivation of the LCT which transforms DDEs with Erlang mixture kernels to ODEs [35].

Lemma F.1. *The approximate system of DDEs obtained by approximating each element of α in (3.1b)–(3.2) with an Erlang mixture approximation can be transformed analytically to the system of ODEs (4.7).*

Proof. Consider the approximate system of DDEs

$$(F.1a) \quad \dot{\hat{x}}(t) = f(\hat{x}(t), \hat{z}(t)),$$

$$(F.1b) \quad \hat{z}(t) = \int_{-\infty}^t \hat{\alpha}(t-s) \odot \hat{r}(s) ds,$$

$$(F.1c) \quad \hat{r}(t) = h(\hat{x}(t)),$$

where each element of the kernel $\hat{\alpha} : \mathbb{R}_{\geq 0}^{n_z} \rightarrow \mathbb{R}^{n_z}$ is an Erlang mixture approximation of α_i (see Proposition 4.2):

$$(F.2) \quad \hat{\alpha}_i(t) = \sum_{m=0}^{M_i} c_{m,i} \ell_{m,i}(t), \quad i = 1, \dots, n_z.$$

The subscript i on the Erlang kernel, $\ell_{m,i} : \mathbb{R}_{\geq 0} \rightarrow \mathbb{R}_{\geq 0}$, indicates that it depends on the i 'th rate parameter, $a_i \in \mathbb{R}_{>0}$. Furthermore, $\hat{x} : \mathbb{R} \rightarrow \mathbb{R}^{n_x}$ and $\hat{z}, \hat{r} : \mathbb{R} \rightarrow \mathbb{R}^{n_z}$ are approximations of x , z , and r , respectively.

First, we introduce the auxiliary memory state $\hat{z}_{m,i} : \mathbb{R} \rightarrow \mathbb{R}$ given by

$$(F.3) \quad \hat{z}_{m,i}(t) = \int_{-\infty}^t \ell_{m,i}(t-s) \hat{r}_i(s) ds, \quad m = 0, \dots, M_i, \quad i = 1, \dots, n_z.$$

Next, we rewrite the expression for the memory state,

$$(F.4) \quad \hat{z}_i(t) = \int_{-\infty}^t \hat{\alpha}_i(t-s) \hat{r}_i(s) ds = \sum_{m=0}^{M_i} c_{m,i} \int_{-\infty}^t \ell_{m,i}(t-s) \hat{r}_i(s) ds = \sum_{m=0}^{M_i} c_{m,i} \hat{z}_{m,i}(t),$$

for $i = 1, \dots, n_z$. The time derivatives of the Erlang kernels are

$$(F.5a) \quad \dot{\ell}_{0,i}(t) = -a_i \ell_{0,i}(t), \quad i = 1, \dots, n_z,$$

$$(F.5b) \quad \dot{\ell}_{m,i}(t) = a_i (\ell_{m-1,i}(t) - \ell_{m,i}(t)), \quad m = 1, \dots, M_i, \quad i = 1, \dots, n_z,$$

and the normalization factor satisfies the recursion

$$(F.6) \quad b_{m,i} = \frac{a_i^{m+1}}{m!} = \frac{a_i}{m} \frac{a_i^m}{(m-1)!} = \frac{a_i}{m} b_{m-1,i}, \quad m = 1, \dots, M_i, \quad i = 1, \dots, n_z.$$

In order to derive differential equations for the auxiliary memory states, we use Leibniz' integral rule [41, Thm. 3, Chap. 8] to differentiate (F.3):

$$(F.7) \quad \dot{\hat{z}}_{m,i}(t) = \ell_{m,i}(0) \hat{r}_i(t) + \int_{-\infty}^t \dot{\ell}_{m,i}(t-s) \hat{r}_i(s) ds, \quad m = 0, \dots, M_i, \quad i = 1, \dots, n_z.$$

Next, we use the time derivatives of the Erlang kernels and the fact that

$$(F.8) \quad \ell_{m,i}(0) = \begin{cases} a_i, & \text{for } m = 0, \\ 0, & \text{for } m = 1, \dots, M_i, \end{cases} \quad i = 1, \dots, n_z,$$

to obtain the differential equations

$$(F.9a) \quad \dot{\hat{z}}_{0,i}(t) = a_i(\hat{r}_i(t) - \hat{z}_{0,i}(t)),$$

$$(F.9b) \quad \dot{\hat{z}}_{m,i}(t) = a_i(\hat{z}_{m-1,i}(t) - \hat{z}_{m,i}(t)), \quad m = 1, \dots, M_i.$$

Finally, by introducing the vector of all memory states,

$$(F.10) \quad \hat{Z} = \begin{bmatrix} \hat{z}_{0,0} \\ \hat{z}_{1,0} \\ \vdots \\ \hat{z}_{M_{n_z}, n_z} \end{bmatrix},$$

the system of DDEs can be transformed to the system of ODEs (4.7). ■

Appendix G. Numerical simulation. In this appendix, we present two numerical methods for simulating DDEs with distributed time delays, i.e., for approximating the solution to initial value problems in the form (3.1)–(3.2). The first is intended for non-stiff systems, and it uses Euler’s explicit method to discretize the differential equations and a left rectangle rule to discretize the integral in the convolution in (3.2a). In contrast, the second is intended for stiff systems, and it uses Euler’s implicit method and a right rectangle rule to discretize the differential equations and the integral, respectively. In both cases, we truncate the integral:

$$(G.1) \quad z(t) = \int_{-\infty}^t \alpha(t-s) \odot r(s) ds \approx \int_{t-\Delta t_h}^t \alpha(t-s) \odot r(s) ds.$$

The memory horizon, $\Delta t_h \in \mathbb{R}_{>0}$, can, e.g., be determined with the bisection approach described in Section 5.1.

G.1. Non-stiff systems. For non-stiff systems, we obtain the approximate system

$$(G.2a) \quad x_{n+1} = x_n + f(x_n, z_n)\Delta t,$$

$$(G.2b) \quad z_{n+1} = \sum_{j=1}^{N_h} \alpha(j\Delta t) \odot r_{n-j+1}\Delta t,$$

$$(G.2c) \quad r_{n+1} = h(x_{n+1}),$$

where $t_n = t_0 + n\Delta t \in \mathbb{R}$ for some time step size, $\Delta t \in \mathbb{R}_{>0}$. We assume that the memory horizon is a multiple, $N_h \in \mathbb{N}$, of the time step size, Δt . For $t_n \leq t_0$, $x_n \in \mathbb{R}^{n_x}$ and $z_n, r_n \in \mathbb{R}^{n_z}$ are equal to $x(t_n)$, $z(t_n)$, and $r(t_n)$, and for $t_n > t_0$, they are approximations. This is an *explicit* approach, i.e., for given values of x_n , z_n , and r_n , z_{n+1} can be computed using (G.2b) and x_{n+1} can be evaluated with (G.2a). Finally, r_{n+1} can be evaluated with (G.2c), and the process is repeated for the subsequent time steps.

G.2. Stiff systems. For stiff systems, the approximate system is

$$(G.3a) \quad x_{n+1} = x_n + f(x_{n+1}, z_{n+1})\Delta t,$$

$$(G.3b) \quad z_{n+1} = \sum_{j=0}^{N_h-1} \alpha(j\Delta t) \odot r_{n-j+1}\Delta t,$$

$$(G.3c) \quad r_{n+1} = h(x_{n+1}),$$

which is a set of algebraic equations that, in general, must be solved numerically. In this work, we solve the residual equation

$$(G.4) \quad R_n(x_{n+1}; x_n) = x_{n+1} - x_n - f(x_{n+1}, z_{n+1})\Delta t = 0,$$

for each time step sequentially. Here, $R_n : \mathbb{R}^{n_x} \times \mathbb{R}^{n_x} \rightarrow \mathbb{R}^{n_x}$ is a residual function, and we consider z_{n+1} and r_{n+1} to be functions of x_{n+1} . Many numerical methods for solving nonlinear equations can utilize the Jacobian of the involved residual function. The Jacobian of the residual function in (G.4) is given by

$$(G.5) \quad \frac{\partial R_n}{\partial x_{n+1}}(x_{n+1}; x_n) = I - \left(\frac{\partial f}{\partial x}(x_{n+1}, z_{n+1}) + \frac{\partial f}{\partial z}(x_{n+1}, z_{n+1}) \frac{\partial z_{n+1}}{\partial x_{n+1}} \right) \Delta t,$$

where $I \in \mathbb{R}^{n_x \times n_x}$ is an identity matrix and the Jacobians of the memory state and the delayed variables are

$$(G.6a) \quad \frac{\partial z_{n+1}}{\partial x_{n+1}} = (\alpha(0)e^T) \odot \frac{\partial r_{n+1}}{\partial x_{n+1}} \Delta t,$$

$$(G.6b) \quad \frac{\partial r_{n+1}}{\partial x_{n+1}} = \frac{\partial h}{\partial x}(x_{n+1}).$$

Here, $e \in \mathbb{R}^{n_z}$ is a column vector of ones.

Appendix H. Kernels in the molten salt reactor model. In this appendix, we describe the kernel in the molten salt nuclear reactor model from Section 7.2. The i 'th kernel, $\alpha_i : \mathbb{R} \rightarrow \mathbb{R}_{\geq 0}$, is given by

$$(H.1) \quad \alpha_i(t) = \gamma_i e^{-\lambda_i t} \sum_{j=1}^{N_s} F(t; \mu_j, \sigma_j), \quad i = 1, \dots, N_g,$$

where $\gamma_i \in \mathbb{R}_{>0}$ is a normalization constant, $F : \mathbb{R}_{\geq 0} \times \mathbb{R} \times \mathbb{R}_{>0} \rightarrow \mathbb{R}_{\geq 0}$ is the folded normal kernel (7.2), and $N_s = 7 \in \mathbb{N}$ is the number of terms. The sum of folded normal kernels represents a nonuniform velocity profile in the external circulation of the molten salt (and neutron precursors), and the second factor describes the decay of the neutron precursors during the external circulation. For given $\mu_1 \in \mathbb{R}$ and $\sigma_1 \in \mathbb{R}_{>0}$, the location and scale parameters are

$$(H.2) \quad \sigma_{j+1} = \frac{3}{2}\sigma_j, \quad \mu_{j+1} = \mu_j + \sigma_j, \quad j = 1, \dots, N_s - 1.$$

Finally, the normalization constant is

(H.3)

$$\gamma_i = \left(\sum_{j=1}^{N_s} \frac{1}{2} e^{\frac{1}{2}\sigma_j^2 \lambda_i^2} \left(e^{\lambda_i \mu_j} \left(1 - \operatorname{erf} \left(\frac{\lambda_i \sigma_j^2 + \mu_j}{\sqrt{2}\sigma} \right) \right) + e^{-\lambda_i \mu_j} \left(1 - \operatorname{erf} \left(\frac{\lambda_i \sigma_j^2 - \mu_j}{\sqrt{2}\sigma_j} \right) \right) \right) \right)^{-1},$$

for $i = 1, \dots, N_g$.